ELSEVIER

Marine Micropaleontology 38 (2000) 119–147

MARINE MICROPALEONTOLOGY

www.elsevier.com/locate/marmicro

Abyssal benthic foraminifera from the northwestern Pacific (Shatsky Rise) during the last 298 kyr

Ken'ichi Ohkushi [a,*], Ellen Thomas [b,c], Hodaka Kawahata [d,e]

[a] *Institute of Geoscience, University of Tsukuba, Tsukuba, Ibaraki, 305-8571, Japan*
[b] *Center for the Study of Global Change, Department of Geology and Geophysics, Yale University, New Haven, CT 06520-8109, USA*
[c] *Department of Earth and Environmental Sciences, Wesleyan University, Middletown, CT 064-0139, USA*
[d] *Geological Survey of Japan, 1-1 Higashi, Tsukuba, Ibaraki, 305-8567, Japan*
[e] *Graduate School of Science, Tohoku University, Sendai, Miyagi, 980-8578, Japan*

Received 9 February 1999; revised version received 3 July 1999; accepted 9 July 1999

Abstract

Benthic foraminifera in a gravity core from Shatsky Rise (northwestern Pacific, water depth 2612 m) show large fluctuations in accumulation rate, species composition and diversity over the last 298 kyr. The most important fluctuations (explaining more than 90% of the faunal variance) result from variations in relative abundance of the three most abundant species: *Epistominella exigua*, *Alabaminella weddellensis* and *Uvigerina peregrina*. High accumulation rates of *U. peregrina*, a species linked to high, continuous productivity, occurred with a 100 kyr periodicity at the end of glacial stages, and correspond to high mass accumulation rates of organic carbon. Peak accumulation rates of *E. exigua* occurred during glacial stage 4 and the middle part of glacial stages 8 and 6, whereas *A. weddellensis* was dominant in the early part of stages 8 and 6, and the late part of stage 3. A high abundance of these species probably indicates lower overall productivity than a high abundance of *U. peregrina*, and their relative and absolute abundances may be linked not simply to the amount of organic matter delivered to the sea floor, but to the intermittent delivery of fresh, easily degraded organic matter. The overall species diversity is negatively correlated to the relative abundance of *E. exigua*, but not to that of *A. weddellensis*, implying that these species have different environmental preferences, although both have been linked to periodic phytodetritus deposition in the present oceans.

Keywords: benthic foraminifera; Shatsky Rise; paleoproductivity; phytodetritus species; Quaternary

1. Introduction

Benthic foraminifera form a major component of the deep-sea meiobenthic communities and of the deep-oceanic biomass (e.g., Gooday et al., 1992; Gooday, 1994, 1999). They possess calcareous tests with a high fossilization potential, and thus can be used in paleoceanographic studies. Studies of North Atlantic benthic foraminifera over the last glacial–interglacial cycle suggested that faunal changes at these time scales were dominantly associated with changes in North Atlantic deep-water circulation (e.g., Schnitker, 1974; Streeter and Shackleton, 1979). More recent studies, however, indicate that the amount and mode of input of organic matter to the sea floor may be a more important determinant of benthic species assemblages (e.g., Corliss and Chen, 1988;

* Corresponding author. Fax: +81 298 51 9764; E-mail: ohkushi@arsia.geo.tsukuba.ac.jp

0377-8398/00/$ – see front matter
PII: S0377-8398(99)00040-7

Gooday, 1988, 1993, 1996, 1999; Corliss, 1991; Loubere, 1991, 1994, 1996, 1998; Rathburn and Corliss, 1994; Schnitker, 1994; Smart et al., 1994; Mackensen et al., 1995; Thomas et al., 1995; Smart and Gooday, 1997; Jannink et al., 1998; Loubere and Fariduddin, 1999). Jorissen et al. (1995) suggested that benthic foraminiferal faunas are dominantly determined by the food supply in more oligotrophic areas, but may be limited by oxygenation in food-rich environments where the oxygen concentration falls below 1 ml/l.

Gooday (1988, 1993) first observed that the abundance of some species of epifaunal benthic foraminifera (including *Alabaminella weddellensis* and *Epistominella exigua*) depends upon a seasonal, thus intermittent flux of phytodetrital material to the sea floor, which reaches the sea floor within a few weeks of its production in surface waters. He suggested that these species, living below overall oligotrophic waters, react opportunistically to an intermittent flux of organic matter, produced during the annual spring bloom at mid-latitudes in the North Atlantic. Such spring bloom conditions do not necessarily lead to high rates of accumulation of organic carbon in the sediments, because labile organic matter is quickly degraded on the sea floor by bacteria and protists in the presence of adequate oxygen (e.g., Turley and Lochte, 1990). Phytodetritus deposition and strong bentho-pelagic coupling was later recognized in many parts of the oceans, including the equatorial Pacific (Smith et al., 1996, 1997).

Loubere (1998) argued that the more common occurrence of the taxa that exploit phytodetritus in the Recent Indian Ocean as compared to the Pacific confirms that they indicate strong seasonality in the flux of food to the ocean floor (see also Loubere and Fariduddin, 1999). Yasuda (1997) described that the abundances of these species and of *Ioanella tumidula* during the late Neogene fluctuated in similar patterns at three sites along a depth transect in the eastern equatorial Atlantic Ocean. These sites are bathed by different water masses, and the abundances of these species were thus not correlated to the physicochemical properties of the bottom waters, but linked to variations in productivity in the surface waters.

Opportunistic taxa which are abundant at highly intermittent phytodetritus fluxes (e.g., *E. exigua*, *A. weddellensis*) have small, thin-walled tests, possessing only a few chambers. Thomas and Gooday (1996) argued that their increased abundance during the Cenozoic may have been caused by the development of the East Antarctic ice sheets in the earliest Oligocene, and the ensuing increased seasonality of surface water productivity at middle and high latitudes in the colder 'icehouse' world.

Taxa with a larger test, more chambers, and living infaunally at various depths in the sediments, such as *Uvigerina* spp., *Globobulimina* spp., and *Bulimina* spp., occur abundantly in regions where the flux of organic matter is high throughout the year (e.g., Lutze and Coulbourn, 1984; Mackensen et al., 1993, 1995; Rathburn and Corliss, 1994; Kitazato and Ohga, 1995; Ohga and Kitazato, 1997; Jannink et al., 1998). Glacial–interglacial changes in the species composition of benthic foraminiferal faunas in various parts of the world's oceans have thus been correlated to changes in productivity, either in total amount of organic matter delivered to the sea floor, or in the pattern of delivery, specifically whether food arrives at the sea floor in a sustained or intermittent pattern (e.g., Thomas et al., 1995; Hermelin and Shimmield, 1995; Schmiedl and Mackensen, 1997). The intermittent delivery results in arrival of fresh, non-degraded organic material, and the character of this organic material may also be of importance to the benthic foraminifera. In addition, the productivity of benthic foraminiferal faunas, expressed in the benthic foraminiferal accumulation rate (BFAR), has been used to estimate overall productivity during glacial times (Herguera and Berger, 1991; Herguera, 1992). The estimates suggested a glacial productivity at low latitudes of about 1.5 to 2 times higher than the present productivity.

Very few data are available on the calcareous benthic foraminifera and glacial–interglacial faunal changes in the northwestern Pacific, because the lysocline in that region is much shallower than in the North Atlantic and a large part of the sea floor therefore lacks carbonate sediment. Shatsky Rise is one of the few exceptions where carbonate sediments can be cored (e.g., core RC10-161, Maiya et al., 1976). This Rise is in the central northwestern Pacific Ocean, mostly below the warm, saline and eastward-flowing Kuroshio Extension, an eastward continuation of the Kuroshio Current, the western boundary current of the North Pacific (e.g., Roden, 1975; Fig. 1). Our coring site is just south of the main path of the

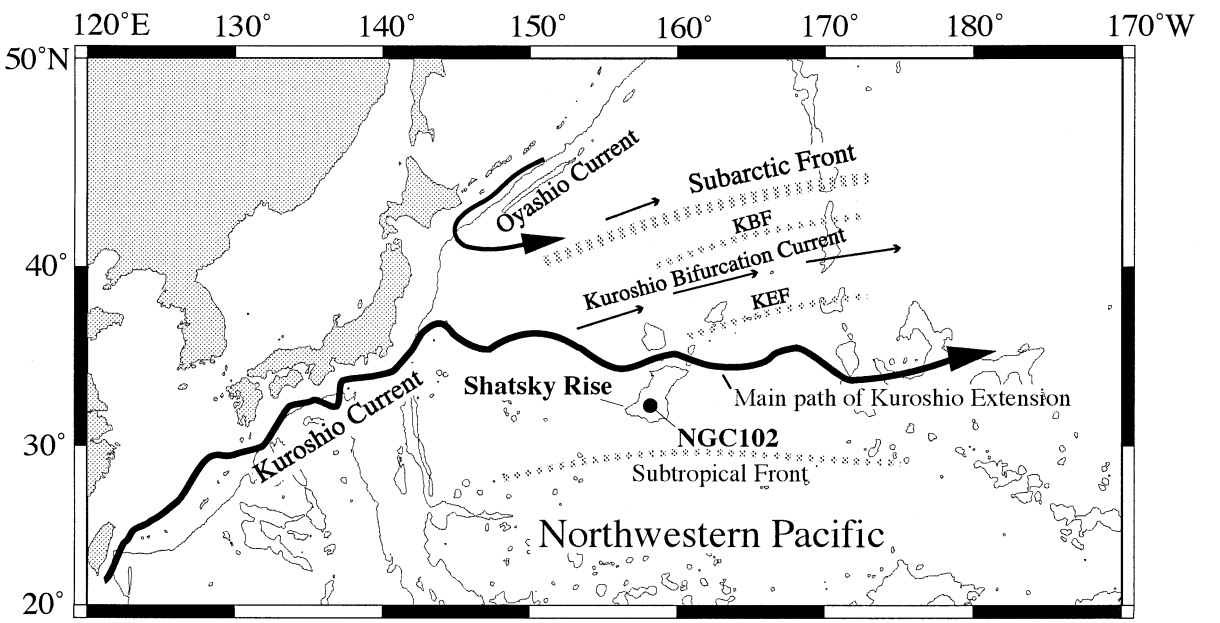

Fig. 1. Location map of core NGC102 in the northwestern Pacific. The position of the main path of the Kuroshio Extension is based on Mizuno and White (1983). The position of the Subarctic front, the KBF (Kuroshio Bifurcation front) and the KEF (Kuroshio Extension front) is based on Zhang and Hanawa (1993).

Kuroshio Extension, but there is considerable annual and interannual variation in the exact location of this current (e.g., Mizuno and White, 1983; Zhang and Hanawa, 1993).

Over Shatsky Rise, the Kuroshio Extension starts to bifurcate, resulting in the existence of various currents separated by frontal zones to the north and east of Shatsky Rise (e.g., Levine and White, 1983; Mizuno and White, 1983). North of the main path of the Kuroshio Extension, the Kuroshio Extension front (KEF) occurs sporadically between latitudes 35° and 37°N (Zhang and Hanawa, 1993). The Subarctic front, recognized as the water mass front between the Kuroshio Extension and the Subarctic waters, is centered near 42–43.5°N. Between the KEF and the Subarctic front, a third front may be associated with the Kuroshio Bifurcation current. Export productivity increases rapidly from the Kuroshio Extension to the Subarctic front (Kawahata et al., 1998).

Steep gradients of biological and physical properties are thus observed in the surface waters in the northwestern Pacific middle latitudes near Shatsky Rise. Thompson and Shackleton (1980) documented at least two prominent southward migrations of the Subarctic front of the northwestern Pacific during glacial episodes of the last 150 kyr: down-core changes in the coiling ratio of *Neogloboquadrina pachyderma* indicate that the front moved from its present position between 42 and 45°N to a location between 35 and 38°N during stage 2, and between 32 and 35°N during stage 6. The rare downcore occurrence of the left coiling *N. pachyderma* in the core used in our study (NGC 102) indicates that the Subarctic front never reached its location at 32°N during the last 298 kyr (de Silva, 1999).

In this study, we will discuss the changes in benthic foraminiferal faunas during the last 298 kyr on Shatsky Rise, and their relation to climate change, with emphasis on changes in paleoproductivity expected to occur as a result of the glacial–interglacial re-organization of the Kuroshio gyre system and the southward advance of the Subarctic front.

2. Material and methods

Gravity core NGC102 (32°19.84′N, 157°51.00′E, water depth 2612 m, length 326 cm) was collected

on Shatsky Rise during cruise NH95-2 of the RV *Hakurei-Maru* (Fig. 1). The carbonate compensation depth (CCD) in the northwestern Pacific is at about 4400 m (Berger et al., 1976), but the lysocline is slightly shallower than 2600 m (de Silva, 1999), suggesting that the core location is presently close to, or slightly below the lysocline. The core consists dominantly of yellowish-brown, homogeneous calcareous ooze. Carbonate contents vary between 38 and 76% with an average of 55% (Kawahata et al., 1999).

Samples (2 cm thick slices) were taken at 4 cm intervals for isotope and foraminiferal study and continuously at 2 cm intervals for the analyses of organic carbon and biogenic opal. The dry bulk density was determined by collecting samples in plastic cubes of 10 cm^3. The dry weight of these samples was determined and divided by the wet volume of the sample to obtain the dry bulk density.

In the laboratory, samples for isotope and foraminiferal study were dried at about 50ºC for two days, weighed, washed through a 63 μm sieve, and dried at 50ºC again. The >63 μm size fraction was weighed and split in two equal parts with a sample splitter. One half was used for faunal analysis, the other for isotope analysis. For both types of analysis samples at 8 cm intervals were used. The initial results of the oxygen isotope analysis, however, resulted in poor resolution in the interval representing marine isotope stages 5 and 7, and for these intervals samples at 4 cm intervals were used to improve the time resolution. The methods of organic carbon and biogenic opal analysis were reported by Kawahata et al. (1999).

An average of 30 specimens of the planktonic foraminifer *Globorotalia inflata* were used in oxygen isotope measurements in 54 samples. We selected specimens from 300 to 355 μm if possible, and in samples with less specimens we extended the size range to >250 μm. Isotope analyses were performed on the Finnigan MAT delta E mass spectrometer at the University of the Ryukyus. External reproducibility of the system was better than 0.05‰. Sample gases were compared to a working standard gas which was regularly calibrated by a NBS-19 reference sample. All the results are expressed in the δ-notation as per mille deviation from the PDB. The oxygen isotopic record was visually correlated to the SPECMAP record (Imbrie et al., 1984) in order to develop an age model (Table 1).

For the benthic foraminiferal analysis we used 44 samples. Samples were dry-sieved using a 75 μm sieve. Many benthic foraminiferal studies in the northwestern Pacific are based on the >75 μm size fraction (Matoba, 1976; Akimoto, 1990; Xu and Ujiié, 1994; Kawagata and Ujiié, 1996), so we decided to use that same size fraction in order to make easy comparisons with those studies. Recent paleoceanographic studies more commonly use the >63 μm size fraction, but in our opinion there are only minor differences in faunas studied in these different size fractions. Larger differences become apparent between these two size fractions and the >125 μm size fraction, because the generally small taxa that use phytodetritus are much less common in the latter size fraction.

We obtained sample splits estimated to contain at least 300 specimens of benthic foraminifera with a microsplitter. All benthic foraminifera were picked from the split, arranged in assemblage slides, identified and counted. Forty-eight species with relative abundances of more than 1% in at least one sample were used in the Q-mode varimax factor analysis of the relative abundance data (Table 2). We used all single species names, but included one group of species, *Stainforthia* spp. (*Stainforthia feylingi* plus *Stainforthia* sp.). We included the *Stainforthia* species in one group because they are minute, show morphological intergradations, and are difficult to distinguish under a binocular microscope. We performed Q-mode factor analysis using a commercially distributed statistics package (SPSS) in order to establish correlations between benthic foraminiferal assemblages and environmental conditions.

We also determined the absolute abundances of benthic foraminifera (number of specimens/gram) and the benthic foraminiferal accumulation rate (BFAR, number of specimens cm^{-2} kyr^{-1}). For this determination all benthic foraminifera in the half sample splits, not only the specimens used in species determination, were counted; usually more than 1000 specimens were present. BFAR was calculated according to:

$$\text{BFAR (number of specimens cm}^{-2}\,\text{kyr}^{-1}) = \text{BF} \times \text{LSR} \times \text{DBD}$$

where BF is the number of benthic foraminifera/gram dry sediment, LSR is the linear sedimentation

Table 1
Oxygen isotope data, linear sedimentation rate (LSR), and dry bulk density (DBD) for core NGC102

Depth in core (cm)	Age (kyr)	Isotopic event	*Globorotalia inflata* $\delta^{18}O$ (‰)	LSR (cm/kyr)	DBD (g/cm^3)
0	0	0	0.52	1.63	0.62
3	1.8		0.22	1.63	0.72
7	4.3		0.21	1.63	0.76
15	9.2		1.08	1.63	0.71
23	14.1		1.59	1.63	0.66
31	19.0	2.2	1.69	1.63	0.62
39	25.8		1.66	1.18	0.68
47	32.6		1.59	1.18	0.76
55	39.4		1.60	1.18	0.73
63	46.2		1.40	1.18	0.78
71	53.0	3.3	1.06	1.18	0.86
79	59.0		1.36	1.33	0.83
87	65.0	4.2	1.43	1.33	0.82
91	71.3		0.94	0.63	0.82
95	77.7		0.92	0.63	0.78
99	84.0		0.88	0.63	0.86
103	90.3		0.88	0.63	0.87
107	96.7		1.08	0.63	0.83
111	103.0		0.97	0.63	0.86
115	109.3		0.91	0.63	0.88
119	115.7		0.70	0.63	0.82
123	122.0	5.5	0.34	0.63	0.83
127	128.5		0.99	0.62	0.8
131	135.0	6.2	1.57	0.62	0.73
139	138.2		1.58	2.50	0.68
147	141.4		1.44	2.50	0.68
155	144.6		1.54	2.50	0.71
163	147.8		1.60	2.50	0.71
171	151.0	6.4	1.72	2.50	0.68
179	156.8		1.38	1.37	0.64
187	162.6		1.38	1.37	0.71
191	165.5		1.29	1.37	0.78
199	171.4		1.51	1.37	0.84
207	177.2		1.66	1.37	0.78
215	183.0	6.6	1.72	1.37	0.72
219	190.5		1.64	0.53	0.75
223	198.0		1.39	0.53	0.77
227	205.5		0.95	0.53	0.83
231	213.0		1.19	0.53	0.8
235	220.5		1.33	0.53	0.8
239	228.0	7.4	1.68	0.53	0.84
243	233.3		1.10	0.76	0.83
247	238.5		1.48	0.76	0.86
251	243.8		1.62	0.76	0.87
255	249.0	8.2	1.85	0.76	0.78
263	254.5		1.73	1.45	0.72
271	260.1		1.81	1.45	0.77
279	265.6		2.12	1.45	0.81
287	271.1		2.13	1.45	0.79
294	275.9		2.16	1.45	0.79
302	281.5		1.78	1.45	0.73
310	287.0	8.5	1.52	1.45	0.79
318	292.5		1.60	1.45	0.74
326	298.1		1.52	1.45	0.67

rate in cm/kyr, and DBD is the dry bulk density (g/cm^3).

Species diversity was calculated from benthic foraminiferal census data using Hurlbert's index (Hurlbert, 1971), because this index is used by many deep-sea workers who use variable sample sizes (Gage and Tyler, 1991). Our sample size fluctuated because the splitting procedure does not always yield splits with exactly 300 specimens, and Hurlbert's index estimates the number of species in a sample of individuals reduced to a common size (m). We determined Hurlbert's diversity index according to:

$$E(S_m) = \sum_{i=1}^{S} \left[1 - C(N - N_i, m)/C(N, m)\right]$$

where $E(S_m)$ is the expected number of species in a sample of m individuals selected at random from a collection containing N individuals (with $m \leq N$), and $C(N-N_i, m) = (N-N_i)!/[m!(N - N_i - m)!]$ for $(N - N_i) \geq m$ and is 0 for $(N - N_i) < m$, $C(N, m) = N!/[m!(N - m)!]$, and N_i is the number of individuals of the ith species (Hurlbert, 1971). We set m at 100, well below the lowest numbers of specimens counted per sample (248).

3. Results

3.1. Oxygen isotope stratigraphy

The isotopic record of core NGC102 agrees in its general features with the SPECMAP time scale (Imbrie et al., 1984) (Fig. 2, Table 1), with the exception of an interval during stage 7 where sedimentation rates, and thus time resolution, are low. The first appearance datum (FAD) of *Emiliania huxleyi*, dated at 260 kyr by Thierstein et al. (1977), occurs at 274 cm corresponding to 263 kyr in our isotope stratigra-

Table 2
Total number of species and total number of specimens picked from each sample, BF (benthic foraminiferal absolute abundance), BFAR (benthic foraminiferal accumulation rate), relative abundances of benthic foraminifera used in a Q-mode factor analysis, and the factor loadings of the first three factors in core NGC102

Age (kyr):	0	4.3	9.2	14.1	19.0	25.8	32.6	39.4	46.2	53.0	59.0	65.0	71.3	84.0	96.7	109.3	122.0	135.0	138.2	141.4	144.6	147.8
Depth in core (cm):	0	7	15	23	31	39	47	55	63	71	79	87	91	99	107	115	123	131	139	147	155	163
Total no. of species:	42	36	57	53	46	43	53	42	33	33	33	41	41	46	46	55	55	46	39	28	29	37
Total no. of specimens picked:	339	261	507	460	424	320	566	550	345	404	682	798	772	602	834	824	454	555	545	499	417	1119
BF:	1721	878	1600	1757	871	1768	1596	1258	1462	1101	2059	3519	2306	1720	1969	1401	754	1998	2700	1495	1371	1582
BFAR:	1733	1085	1860	1897	883	1416	1435	1075	1338	1110	2276	3835	1187	931	1031	776	397	897	3050	1698	1633	1873
Alabaminella weddelensis	5.0	1.9	4.7	14.3	20.3	27.3	25.4	13.9	12.4	5.7	4.3	4.5	3.0	2.2	3.8	4.8	1.5	2.9	2.9	3.4	3.6	7.7
Brizalina translucens	2.1	1.9	2.5	4.1	3.8	2.8	2.5	0.7	0.0	0.2	0.1	0.5	0.4	0.7	0.4	0.7	2.6	5.7	6.0	4.0	2.9	0.6
Bulimina aculeata	0.0	0.0	0.0	0.0	0.0	0.0	0.0	0.0	0.0	0.0	0.0	0.0	0.0	0.2	0.0	0.2	1.1	0.4	0.0	0.0	0.0	0.0
Bulimina striata	0.6	0.8	1.0	0.2	0.5	0.0	0.0	0.0	0.0	0.0	0.0	0.0	0.0	0.0	0.1	0.0	0.9	0.9	0.7	0.0	0.0	0.0
Cassidulina carinata	2.9	1.5	5.9	5.0	3.8	3.4	4.7	4.0	2.0	0.7	1.0	0.0	0.0	0.2	0.0	0.0	0.0	1.1	0.5	0.0	0.0	0.0
Cassidulina norvangi	2.4	0.4	2.0	5.2	6.6	3.7	3.5	4.7	4.6	0.7	3.7	1.4	2.7	1.5	2.5	2.3	6.8	7.4	10.4	9.8	8.4	11.8
Chilostomella oolina	0.0	0.0	0.2	0.0	0.5	0.0	0.0	0.0	0.3	0.0	0.0	0.0	0.0	0.0	0.1	0.0	0.0	1.3	3.3	0.2	0.0	0.0
Cibicides sp. 1	0.6	1.1	1.8	1.9	5.2	5.6	5.1	2.7	2.0	1.0	1.0	0.5	0.8	1.2	1.0	0.8	1.3	0.0	0.5	0.2	0.5	0.5
Cibicidoides bradyi	1.8	0.8	0.6	0.0	0.0	0.0	0.0	0.0	0.0	0.0	0.0	0.0	0.0	0.0	0.0	0.0	0.0	0.0	0.0	0.0	0.0	0.0
Cibicidoides cicatricosus	0.0	0.0	0.0	0.0	0.0	0.6	0.0	0.4	0.0	0.7	0.0	0.0	0.0	0.0	0.0	0.8	0.9	0.2	0.4	0.4	0.5	0.6
Cibicidoides mundulus	0.0	0.0	0.0	0.0	0.0	0.0	0.0	0.0	0.0	0.0	0.1	0.0	0.0	0.0	0.0	0.0	0.0	0.0	0.0	0.0	0.0	0.0
Epistominella exigua	36.0	22.6	12.3	12.3	4.2	9.3	11.9	36.6	49.7	62.6	70.8	70.8	71.4	61.8	63.7	63.0	34.9	16.0	20.8	57.1	54.0	61.3
Eponides lamarckianus	0.0	0.0	0.2	0.2	0.0	0.3	0.9	0.7	0.6	1.0	0.0	0.3	0.8	0.8	0.8	0.5	0.2	0.2	0.4	0.8	0.2	0.1
Eponides sp. 1	0.0	0.0	0.4	0.4	0.9	0.3	0.5	0.7	0.3	0.5	0.1	0.1	0.4	0.0	0.0	0.1	0.0	0.4	0.0	0.0	0.2	0.4
Eponides tenerus	2.9	2.7	2.5	6.5	2.6	3.7	2.5	1.4	0.9	0.7	0.1	0.0	0.0	0.0	0.7	1.1	0.2	0.0	0.4	1.2	2.9	2.2
Evolvocassidulina brevis	0.9	0.4	0.0	0.0	0.0	0.0	0.0	0.0	0.0	0.0	0.0	0.1	0.0	0.3	0.0	0.7	2.0	0.0	0.0	0.0	0.0	0.0
Evolvocassidulina tenuis	0.0	0.0	0.0	0.0	0.0	0.0	0.0	0.0	0.0	0.0	0.0	0.0	0.0	0.0	0.0	0.2	0.0	0.4	0.7	0.0	0.0	0.0
Favocassidulina favus	0.9	1.1	0.0	0.0	0.0	0.0	0.0	0.0	0.0	0.0	0.0	0.0	0.0	0.0	0.0	0.0	0.0	0.0	0.0	0.0	0.0	0.0
Fissurina abyssicola	0.0	0.0	0.0	0.2	0.0	0.0	1.1	0.0	0.0	0.0	0.0	0.0	0.0	0.0	0.0	0.0	0.0	0.0	0.0	0.0	0.0	0.0
Fissurina sp. 1	0.0	0.4	0.2	0.0	0.5	0.3	0.0	0.0	0.3	0.5	0.1	0.8	1.0	0.5	0.4	0.6	0.0	0.0	0.0	0.0	0.0	0.1
Fissurina abyssicola	0.0	0.0	0.0	0.2	0.0	0.0	1.1	0.0	0.0	0.0	0.0	0.0	0.0	0.0	0.0	0.0	0.0	0.0	0.0	0.0	0.0	0.0
Fissurina sp. 1	0.0	0.4	0.2	0.0	0.5	0.3	0.0	0.0	0.3	0.5	0.1	0.8	1.0	0.5	0.4	0.6	0.0	0.0	0.0	0.0	0.0	0.1
Francesita advena	0.0	0.4	0.0	0.0	0.7	0.0	1.4	0.2	0.9	0.2	0.1	0.8	0.8	1.5	0.4	0.6	2.2	0.0	0.0	0.0	0.0	0.0
Fursenkoina cedrosensis	5.0	5.0	1.4	0.6	0.0	0.0	0.2	0.0	0.0	0.2	0.0	0.0	0.3	0.0	0.1	0.2	0.9	0.0	0.0	0.0	0.0	0.0
Globocassidulina subglobosa	5.6	5.4	3.1	5.2	8.5	5.3	6.3	3.8	4.6	3.0	3.4	0.9	3.0	1.7	2.5	3.6	3.3	1.8	1.3	3.2	2.9	6.0
Gyroidina kawagatai	0.9	1.5	1.2	1.3	0.7	0.0	1.4	1.1	0.0	0.5	0.4	0.1	0.4	0.2	1.0	0.6	0.9	0.2	0.4	0.0	0.0	0.0
Gyroidina sp. 1	1.5	0.4	0.0	0.2	0.0	0.0	0.0	0.0	0.0	0.0	0.0	0.0	0.0	0.0	0.0	0.1	0.4	0.0	0.0	0.0	0.0	0.0

Table 2 (continued)

Age (kyr):	0	4.3	9.2	14.1	19.0	25.8	32.6	39.4	46.2	53.0	59.0	65.0	71.3	84.0	96.7	109.3	122.0	135.0	138.2	141.4	144.6	147.8
Depth in core (cm):	0	7	15	23	31	39	47	55	63	71	79	87	91	99	107	115	123	131	139	147	155	163
Total no. of species:	42	36	57	53	46	43	53	42	33	33	33	41	41	46	46	55	55	46	39	28	29	37
Total no. of specimens picked:	339	261	507	460	424	320	566	550	345	404	682	798	772	602	834	824	454	555	545	499	417	1119
BF:	1721	878	1600	1757	871	1768	1596	1258	1462	1101	2059	3519	2306	1720	1969	1401	754	1998	2700	1495	1371	1582
BFAR:	1733	1085	1860	1897	883	1416	1435	1075	1338	1110	2276	3835	1187	931	1031	776	397	897	3050	1698	1633	1873
Ioanella tumidula	0.6	0.0	0.0	0.0	0.0	0.0	1.2	0.5	0.3	0.2	0.3	0.0	0.3	0.2	0.1	0.8	2.2	1.8	0.2	0.0	0.0	0.0
Lagena sp.	0.0	0.0	0.0	0.0	0.0	0.0	0.2	0.0	0.3	0.0	0.0	0.0	0.0	0.0	0.0	0.1	0.0	0.0	0.0	0.0	0.0	0.0
Lagenammina atlantica	1.2	0.0	0.0	0.0	0.0	0.0	0.0	0.0	0.0	0.0	0.0	0.0	0.0	0.0	0.0	0.0	0.0	0.0	0.0	0.0	0.0	0.0
Melonis barleeanum	0.9	0.8	2.0	3.7	3.5	4.3	1.1	0.0	0.0	0.0	0.0	0.0	0.0	0.0	0.0	0.2	0.2	0.7	1.1	2.0	1.7	1.4
Melonis sphaeroides	0.0	0.0	0.0	0.2	0.2	0.0	0.2	0.4	0.0	0.0	0.0	0.0	0.0	0.0	0.1	0.0	0.0	0.2	0.9	0.0	0.0	0.0
Oolina globosa	0.3	1.1	0.0	0.0	0.2	0.3	0.4	0.0	0.0	0.0	0.0	0.0	0.4	0.2	0.1	0.0	0.0	0.0	0.0	0.0	0.0	0.0
Oridorsalis umbonatus	0.3	0.8	2.9	1.9	5.2	6.2	5.6	6.2	1.2	4.0	2.1	2.5	3.9	4.5	3.1	3.4	1.7	0.2	0.4	0.4	0.2	0.2
Pacinonion novozealandicum	0.0	0.0	1.0	2.2	3.3	5.9	7.7	7.8	3.8	1.7	1.9	2.0	1.0	1.3	2.4	0.5	0.9	1.6	0.9	3.4	1.2	1.9
Parafissurina lateralis	0.3	0.0	0.0	0.0	0.0	0.0	0.2	0.2	1.2	0.0	0.1	0.1	0.0	0.0	0.1	0.0	0.0	0.0	0.0	0.0	0.0	0.1
Planulina wuellerstorfi	0.6	2.3	2.9	2.6	7.1	7.5	5.6	2.7	2.3	4.2	2.8	3.5	1.9	2.5	2.5	3.0	0.4	0.9	0.9	1.6	1.0	1.2
Pullenia bolloides	0.0	1.9	1.6	0.0	0.0	0.3	0.0	0.0	0.0	0.0	0.0	0.0	0.4	0.3	0.1	0.4	2.2	0.2	0.0	0.0	0.0	0.0
Pullenia okinawaensis	0.0	0.0	0.4	0.2	0.0	0.0	0.0	0.2	0.0	0.0	0.7	0.4	0.6	0.3	0.7	0.7	0.4	0.0	0.2	0.2	0.2	0.1
Pullenia quinqueloba	0.3	0.0	0.4	0.2	1.2	0.3	2.1	3.4	1.4	2.0	0.9	1.3	1.0	1.8	0.8	0.4	1.5	0.4	0.4	0.0	0.2	0.1
Pulleniella asymmetrica	0.9	0.0	0.2	0.4	0.0	0.0	0.0	0.0	0.0	0.0	0.0	0.0	0.0	0.0	0.0	0.2	0.7	0.0	0.0	0.0	0.0	0.0
Pyrgo murrhina	0.0	0.0	0.8	0.0	0.2	0.0	0.0	0.0	0.0	0.0	0.0	0.0	0.0	0.0	0.0	0.0	0.0	0.0	0.0	0.0	0.0	0.0
Pyrgo oblonga	0.0	0.0	0.2	0.2	0.2	0.0	0.2	0.0	0.0	0.0	0.0	0.0	0.0	0.0	0.0	0.0	0.2	1.4	2.4	0.0	1.0	0.0
Quadrimorphina laevigata	0.9	0.4	1.8	1.5	0.2	0.0	0.0	0.0	0.0	0.2	0.0	0.0	0.0	0.0	0.0	0.5	2.4	4.5	3.5	0.0	0.0	0.0
Reophax cf. *guttifer*	1.2	0.0	0.0	0.0	0.0	0.0	0.0	0.0	0.0	0.0	0.0	0.0	0.0	0.0	0.0	0.0	0.0	0.0	0.0	0.0	0.0	0.0
Stainforthia complanata	2.1	1.1	0.8	0.9	0.7	0.9	0.7	0.5	0.6	0.5	0.3	0.8	0.1	0.5	0.4	0.5	1.3	2.2	1.8	2.0	1.9	0.9
Stainforthia spp.	0.0	1.1	3.1	3.7	2.4	0.9	0.4	0.0	0.0	0.5	0.1	0.0	0.1	0.0	0.4	0.0	0.0	0.5	0.7	0.0	0.0	0.1
Triloculina frigida	0.0	0.0	0.0	0.2	1.2	0.9	0.4	0.2	0.0	0.0	0.0	0.3	0.0	0.0	0.0	0.0	0.0	0.7	0.4	0.0	0.0	0.2
Uvigerina peregrina	15.9	37.5	34.8	17.5	9.0	1.9	0.5	2.4	5.8	5.7	3.1	5.3	2.1	11.1	8.5	4.2	16.1	41.8	34.9	7.8	14.1	0.9
Valvulineria cf. *minuta*	0.0	0.0	0.8	0.4	0.0	0.0	0.4	0.4	0.3	0.0	0.0	0.0	0.0	0.0	0.0	0.0	1.1	0.4	0.5	0.0	0.0	0.0
Factor 1	0.84	0.40	0.19	0.31	0.02	0.19	0.30	0.87	0.93	0.97	0.98	0.98	0.98	0.96	0.96	0.97	0.85	0.23	0.38	0.95	0.92	0.96
Factor 2	0.16	0.04	0.10	0.56	0.88	0.94	0.92	0.42	0.29	0.15	0.12	0.11	0.10	0.08	0.11	0.13	0.06	0.02	0.03	0.11	0.11	0.19
Factor 3	0.48	0.88	0.94	0.72	0.39	0.08	0.04	0.14	0.21	0.17	0.14	0.16	0.12	0.26	0.22	0.16	0.51	0.96	0.90	0.25	0.36	0.14

Table 2 (continued)

Age (kyr):	151.0	156.8	162.6	165.5	171.4	177.2	183.0	198.0	213.0	228.0	238.5	249.0	254.5	260.1	265.6	271.1	275.9	281.5	287.0	292.5	298.1
Depth in core (cm):	171	179	187	191	199	207	215	223	231	239	247	255	263	271	279	287	294	302	310	318	326
Total no. of species:	26	27	32	31	35	39	49	52	44	49	59	40	39	41	44	43	39	38	50	36	47
Total no. of specimens picked:	248	345	460	430	471	441	603	491	972	672	635	333	487	586	620	341	354	384	713	499	573
BF:	1716	1155	1177	1071	992	921	555	709	1148	807	291	1109	1454	1027	777	553	484	547	458	703	460
BFAR:	1941	1241	1396	1394	1662	1437	801	290	489	359	191	659	1509	1149	913	634	551	576	526	753	448
Alabaminella weddelensis	4.8	3.5	10.0	22.8	23.3	28.8	23.4	11.4	2.9	5.8	8.3	3.9	1.8	1.7	1.6	1.2	0.6	18.7	27.3	43.0	41.1
Brizalina translucens	2.0	2.6	0.4	0.9	1.5	1.1	1.6	2.6	0.5	0.7	2.7	1.2	3.3	1.7	4.0	2.3	2.8	2.6	3.4	4.6	2.6
Bulimina aculeata	0.0	0.0	0.0	0.0	0.0	0.0	0.0	0.0	1.1	3.4	5.2	7.5	0.0	0.0	0.0	0.0	0.0	0.3	0.0	0.0	0.0
Bulimina striata	0.0	0.0	0.0	0.0	0.0	0.0	0.0	0.4	0.0	0.3	0.6	1.2	0.0	0.0	0.0	0.0	0.0	0.0	0.0	0.0	0.0
Cassidulina carinata	0.0	0.0	0.2	0.0	0.0	0.0	0.0	0.0	0.0	0.0	0.0	0.0	0.0	0.0	0.0	0.0	0.0	0.0	0.0	0.0	0.0
Cassidulina norvangi	10.5	10.7	5.4	0.0	1.1	0.5	1.2	0.8	1.4	3.3	8.9	12.5	12.3	1.7	4.3	2.6	1.7	1.8	1.3	1.8	1.2
Chilostomella oolina	0.0	0.0	0.7	0.0	0.0	0.2	0.0	0.6	0.0	0.0	0.3	1.5	0.2	1.2	0.3	0.3	0.3	0.0	0.3	0.0	0.2
Cibicides sp. 1	2.0	0.3	2.6	0.9	1.7	1.4	2.3	3.2	0.9	1.2	1.3	1.2	1.6	2.2	2.6	3.2	6.8	1.8	4.2	2.0	3.3
Cibicidoides bradyi	0.0	0.0	0.0	0.0	0.0	0.0	0.0	0.0	0.0	0.0	0.0	0.0	0.0	0.0	0.0	0.0	0.0	0.0	0.0	0.0	0.0
Cibicidoides cicatricosus	0.8	1.4	0.0	0.0	0.6	0.0	0.0	0.0	0.0	0.0	0.0	0.0	0.0	0.0	0.0	0.0	0.0	0.0	0.0	0.0	0.0
Cibicidoides mundulus	0.0	0.0	0.0	0.0	0.0	0.0	0.2	0.4	0.1	1.0	0.2	0.0	0.0	0.0	0.3	0.9	0.3	0.5	0.6	0.0	0.0
Epistominella exigua	48.4	57.1	56.1	42.3	44.1	26.1	20.9	28.4	61.2	28.1	10.6	5.1	32.2	51.2	40.4	39.1	33.3	35.2	11.9	2.6	1.9
Eponides lamarckianus	0.0	0.0	1.3	0.0	0.4	0.9	2.6	1.4	1.3	1.5	0.2	0.9	0.2	0.2	0.0	0.0	0.0	0.0	0.0	0.4	0.7
Eponides sp. 1	0.4	0.0	0.0	0.0	0.2	0.9	0.0	0.4	0.1	0.3	1.6	2.4	3.7	0.5	2.1	0.9	0.0	0.0	0.0	0.0	0.0
Eponides tenerus	1.6	3.8	3.0	2.1	2.1	3.2	1.0	1.8	0.1	0.9	2.8	3.6	3.7	3.9	2.6	2.9	2.8	7.0	4.8	5.4	4.3
Evolvocassidulina brevis	0.0	0.0	0.2	1.2	0.4	0.9	0.7	0.2	0.1	0.4	0.0	0.3	0.0	0.0	0.0	0.0	0.0	0.0	0.0	0.0	0.0
Evolvocassidulina tenuis	0.0	0.0	0.0	0.0	0.0	0.0	0.0	0.0	0.0	0.0	0.0	0.0	0.2	2.0	0.8	0.6	0.3	0.0	0.4	0.0	1.9
Favocassidulina favus	0.0	0.0	0.0	0.0	0.0	0.0	0.0	0.0	0.0	0.0	0.0	0.0	0.0	0.0	0.0	0.0	0.0	0.0	0.0	0.0	0.0
Fissurina abyssicola	0.0	0.0	0.0	0.0	0.0	0.0	0.0	0.0	0.0	0.0	0.0	0.0	0.0	0.0	0.0	0.0	0.0	0.0	0.0	0.0	0.0
Fissurina sp. 1	0.0	0.0	0.0	0.0	0.0	0.0	0.0	0.0	0.1	0.1	0.2	0.3	0.0	0.0	0.2	0.9	1.4	0.0	0.0	0.0	0.0
Francesita advena	0.0	0.0	0.2	0.2	0.0	0.7	0.5	1.6	1.3	0.9	0.5	1.2	0.8	3.8	2.9	2.9	4.5	0.5	2.2	1.4	2.3
Fursenkoina cedrosensis	0.0	0.0	0.0	0.0	0.0	0.0	0.2	0.6	0.7	0.4	0.5	0.0	0.0	0.2	0.0	0.3	0.0	0.3	2.9	0.4	0.3
Globocassidulina subglobosa	4.0	5.5	2.8	11.2	4.0	7.3	10.2	7.3	9.5	6.2	13.6	9.0	17.0	7.3	15.3	12.2	10.2	13.0	14.4	17.6	16.1
Gyroidina kawagatai	0.0	0.0	0.0	0.2	0.0	0.0	0.0	0.0	0.0	0.9	0.5	0.0	0.4	0.2	0.3	0.3	0.6	0.3	0.1	0.0	0.3
Gyroidina sp. 1	0.0	0.0	0.0	0.0	0.0	0.0	0.0	0.0	0.0	0.0	0.0	0.0	0.0	0.0	0.0	0.0	0.0	1.0	1.1	0.8	0.3

Table 2 (continued)

Age (kyr):	151.0	156.8	162.6	165.5	171.4	177.2	183.0	198.0	213.0	228.0	238.5	249.0	254.5	260.1	265.6	271.1	275.9	281.5	287.0	292.5	298.1
Depth in core (cm):	171	179	187	191	199	207	215	223	231	239	247	255	263	271	279	287	294	302	310	318	326
Total no. of species:	26	27	32	31	35	39	49	52	44	49	59	40	39	41	44	43	39	38	50	36	47
Total no. of specimens picked:	248	345	460	430	471	441	603	491	972	672	635	333	487	586	620	341	354	384	713	499	573
BF:	1716	1155	1177	1071	992	921	555	709	1148	807	291	1109	1454	1027	777	553	484	547	458	703	460
BFAR:	1941	1241	1396	1394	1662	1437	801	290	489	359	191	659	1509	1149	913	634	551	576	526	753	448
Ioanella tumidula	0.0	0.0	0.0	0.9	0.2	0.2	0.7	0.4	0.4	0.4	0.9	0.0	0.2	0.3	0.2	0.0	0.0	0.3	0.4	0.2	0.0
Lagena sp.	0.0	0.0	0.0	0.0	0.0	0.0	0.0	0.0	0.0	0.0	0.0	0.0	0.0	0.0	0.0	0.9	1.1	0.3	0.0	0.0	0.0
Lagenammina atlantica	0.0	0.0	0.0	0.0	0.0	0.0	0.0	0.0	0.0	0.0	0.0	0.0	0.0	0.0	0.0	0.0	0.0	0.0	0.0	0.0	0.0
Melonis barleeanum	1.6	1.4	2.0	2.3	2.8	4.1	0.7	0.0	0.5	0.1	0.8	1.2	0.0	0.0	0.0	0.0	0.3	0.0	0.0	0.0	0.0
Melonis sphaeroides	0.0	0.0	0.0	0.0	0.2	0.2	0.2	0.4	0.0	0.1	0.8	0.9	1.4	0.0	0.0	0.0	0.0	0.0	0.0	0.0	0.0
Oolina globosa	0.0	0.3	0.0	0.5	0.2	0.2	0.0	0.0	0.0	0.1	0.0	0.6	0.2	0.0	0.0	0.0	0.3	0.0	0.0	0.0	0.0
Oridorsalis umbonatus	0.0	0.0	0.7	0.9	0.6	0.9	1.6	1.4	0.8	1.8	1.7	0.9	0.8	0.9	0.6	0.9	1.4	3.4	6.3	3.0	4.5
Pacinonion novozealandicum	2.4	0.6	4.3	1.9	2.5	5.4	7.1	3.9	3.9	3.1	1.3	1.2	2.7	4.9	1.4	0.0	0.0	0.0	1.0	1.8	2.4
Parafissurina lateralis	0.4	0.3	0.2	0.2	0.0	0.2	0.0	0.4	0.2	0.0	0.2	0.0	0.0	0.0	0.0	0.6	0.0	0.0	0.1	0.0	0.0
Planulina wuellerstorfi	1.2	0.6	3.3	3.3	2.8	1.1	2.0	3.4	0.5	2.1	1.4	0.6	1.6	1.4	3.4	3.8	3.4	3.9	8.0	4.6	4.2
Pullenia bolloides	0.0	0.0	0.4	0.0	0.2	0.0	0.0	0.4	0.8	0.9	1.7	1.5	2.9	0.7	1.6	4.4	3.4	1.0	0.1	0.2	0.2
Pullenia okinawaensis	0.0	0.0	0.0	0.2	0.2	0.2	0.3	0.8	0.1	0.6	1.1	0.6	0.0	0.2	0.2	0.6	0.6	0.8	0.4	0.6	0.3
Pullenia quinqueloba	0.8	0.9	0.4	0.0	0.4	0.2	1.2	2.6	0.3	1.3	0.6	0.6	0.6	0.9	0.5	1.2	1.4	0.3	1.1	1.0	0.5
Pulleniella asymmetrica	0.0	0.0	1.5	4.0	5.9	9.5	12.5	11.8	4.3	3.6	3.1	1.2	0.4	0.0	0.0	0.0	0.3	0.0	0.0	0.0	0.0
Pyrgo murrhina	1.2	0.3	0.0	0.0	0.0	0.0	0.0	0.0	0.0	0.0	0.0	0.0	0.0	0.5	0.0	0.0	0.0	0.0	0.0	0.0	0.0
Pyrgo oblonga	1.2	0.0	0.0	0.0	0.0	0.0	0.3	0.0	0.1	0.1	0.6	0.6	0.2	0.2	0.0	0.3	0.3	0.0	0.0	0.0	0.0
Quadrimorphina laevigata	0.0	0.0	0.2	0.0	0.0	0.0	0.0	0.0	0.2	1.5	4.2	3.3	0.6	2.4	1.6	0.3	0.0	0.0	0.0	0.0	0.2
Reophax cf. *guttifer*	0.0	0.0	0.0	0.0	0.0	0.0	0.0	0.0	0.0	0.0	0.0	0.0	0.0	0.0	0.0	0.0	0.0	0.0	0.0	0.0	0.0
Stainforthia complanata	0.8	1.7	1.3	0.7	1.7	2.0	1.3	0.4	0.9	1.3	1.1	1.5	3.3	1.2	1.8	1.5	0.8	0.5	0.8	1.0	0.9
Stainforthia spp.	0.4	0.3	0.2	0.0	0.0	0.2	0.3	2.4	1.0	0.7	2.8	2.7	0.4	0.9	1.1	0.3	1.1	0.0	0.3	0.8	1.0
Triloculina frigida	0.4	0.0	0.0	0.2	0.2	0.0	0.2	0.0	0.1	0.1	0.3	0.0	0.4	0.2	0.6	2.9	4.8	0.3	0.0	0.0	0.0
Uvigerina peregrina	12.1	5.8	0.4	0.0	0.4	0.5	1.3	3.7	2.6	22.9	13.4	26.9	3.9	4.3	5.6	6.4	11.3	1.6	1.0	2.6	3.3
Valvulineria cf. *minuta*	0.0	0.0	0.0	0.0	0.2	0.0	0.2	0.4	0.0	0.1	0.8	0.6	0.2	0.0	0.0	0.0	0.0	0.3	0.0	0.0	0.3
Factor 1	0.91	0.96	0.96	0.82	0.84	0.58	0.54	0.81	0.98	0.68	0.32	0.02	0.83	0.97	0.91	0.92	0.86	0.80	0.26	−0.04	−0.05
Factor 2	0.14	0.12	0.23	0.54	0.51	0.76	0.76	0.44	0.13	0.19	0.46	0.13	0.21	0.12	0.18	0.14	0.12	0.56	0.93	0.98	0.98
Factor 3	0.35	0.22	0.11	0.08	0.08	0.05	0.07	0.17	0.14	0.69	0.69	0.94	0.27	0.18	0.26	0.26	0.39	0.14	0.07	0.08	0.08

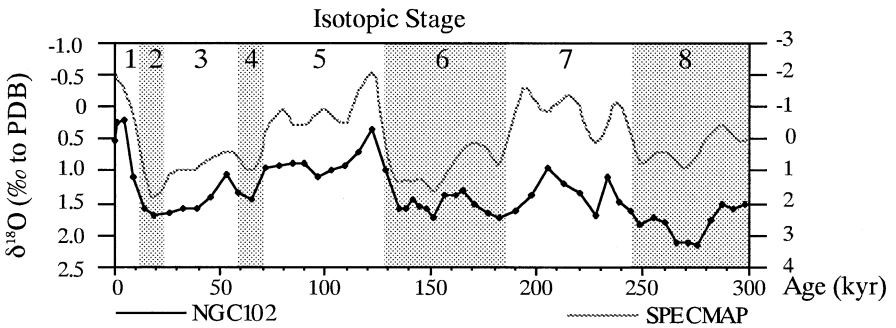

Fig. 2. Time series plot of $\delta^{18}O$ (‰) for *Globorotalia inflata* in NGC102 superimposed on the SPECMAP global stack (Imbrie et al., 1984) for the past 298 kyr. The isotopic variation in the SPECMAP stack is expressed in standard deviation units around a zero mean. The age model is given in Table 1.

phy (Tanaka, 1996). The last down-core occurrence of *Globigerinoides ruber* pink occurs at 119 cm, consistent with the timing of its disappearance in the Pacific at approximately 122 kyr (Thompson et al., 1979).

The mass accumulation rate of bulk sediments (MARsediment) was calculated by multiplying the estimated linear sedimentation rate by the dry bulk density (Fig. 3), and ranges between 0.4 and 1.8 g cm^{-2} kyr^{-1}. Glacial values (mean 1.1 g cm^{-2} kyr^{-1}) are approximately 1.7 times higher than interglacial values (mean 0.6 g cm^{-2} kyr^{-1}). The highest values (1.7–1.8 g cm^{-2} kyr^{-1}) occurred during the later part of stage 6.

Using our age model results in a large difference of the MARsediment in stages 6 and 7. This difference could be an artifact resulting from problems in the age model: our isotope curve differs somewhat from the SPECMAP curve in stage 7 to early stage 6 (Fig. 2). We do not believe, however, that this is the case: isotopic event 6.6 near the stage boundary and isotopic event 6.4 in the middle part of stage 6 are well defined. In addition, the position of the stage 6/stage 7 boundary corresponds approximately to the timing of surface water cooling as estimated from the planktonic foraminiferal fauna (de Silva, 1999), and the MARsediment for stage 7 is comparable to that for stage 5.

We think that the large differences between the MARsediment in stages 6 and 7 are real, with maximum values late in stage 6, at least in part because productivity may have been very high during glacial stage 6 (Thompson and Shackleton, 1980), as also seen in the MARsediment in core NGC102. In addition, the low MARsediment in stage 7 might have been influenced by carbonate dissolution. Downcore variations in carbonate dissolution were expressed in the dissolution index which reflects fragmentation of foraminifera according to:

$$\mathrm{FRAG} = \frac{(\text{number of foraminiferal fragments})}{(\text{number of foraminiferal fragments} + \text{number of whole foraminiferal test})}$$

(Fig. 3; de Silva (1999)).

The dissolution index increases during the early part of stages 8, 7, and the middle part of stage 5, showing generally higher dissolution rates during interglacials. Thus, the lower MARsediment during interglacial stages (including stage 7) may be due to the combined effects of an increase in carbonate dissolution and a decrease in biogenic and lithogenic flux. We thus feel confident that our estimates of MARsediment in stages 6 and 7 reflect the true overall trends in sedimentation.

3.2. Organic carbon and biogenic opal

The organic carbon content varies between 0.2 and 0.73 wt.%, with an average of 0.43% (Kawahata et al., 1999). Values are generally higher for glacial intervals, with peak values towards the end of the glacials at a cyclicity of about 100 kyr (Fig. 3). The mass accumulation rate (MAR) of organic carbon (C_{org}) varies between 1.5 and 7.9 mg cm^{-2} kyr^{-1} (Fig. 3), and is higher during glacial intervals. The MARsediment and the C_{org} percentage are both higher during glacial intervals, so that MAR of C_{org} is markedly

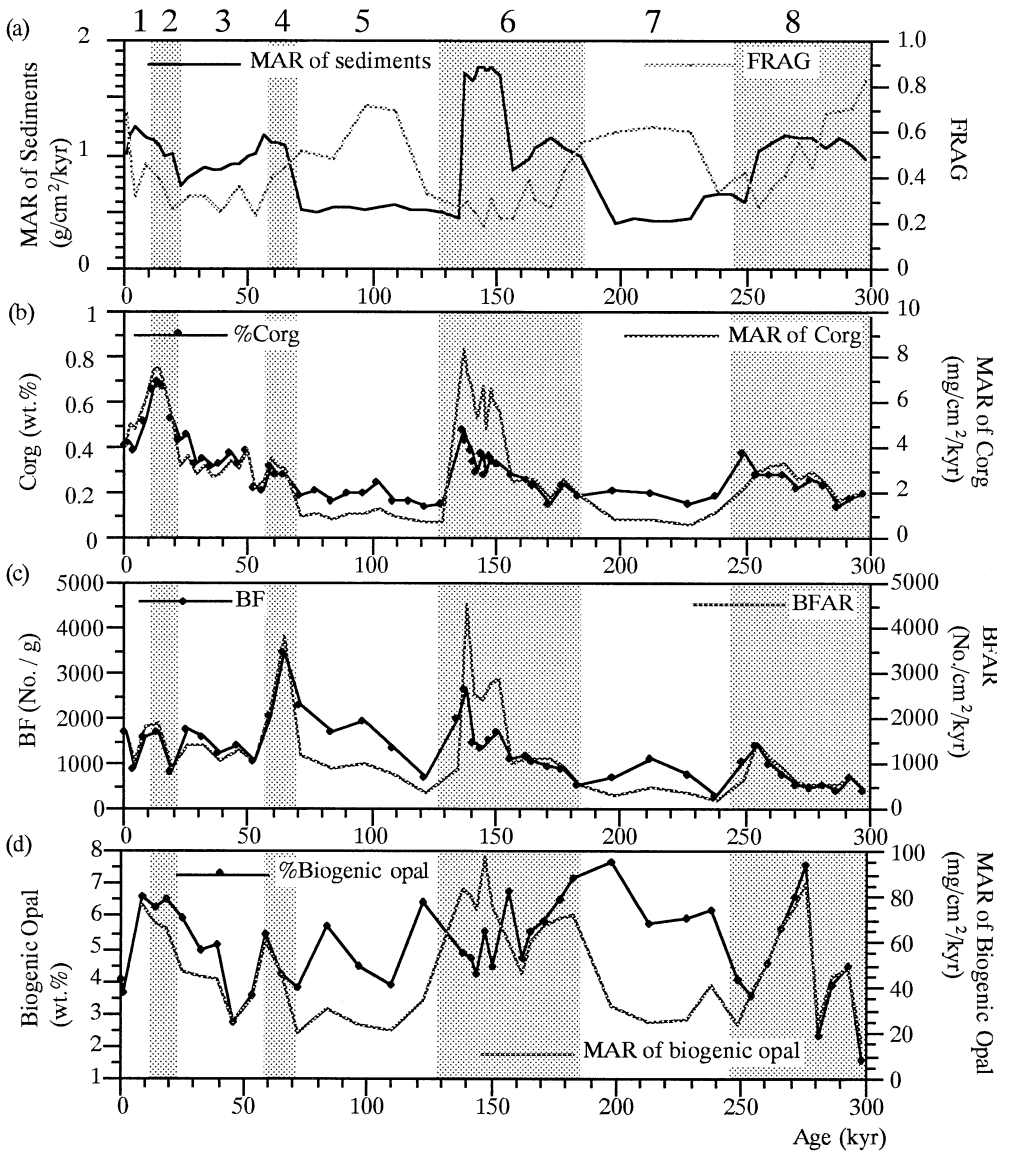

Fig. 3. Time series plots of (a) the mass accumulation rate (MAR) of sediments and the relative proportion of foraminiferal fragments (*FRAG*), (b) the organic carbon (C_{org}) content and the mass accumulation rate (MAR) of C_{org}, (c) the absolute abundance of benthic foraminifera (BF) and the benthic foraminiferal accumulation rate (BFAR), and (d) the biogenic opal content and MAR of biogenic opal. FRAG after de Silva (1999); data on C_{org} and biogenic opal after Kawahata et al. (1999).

higher during glacials. Particularly high values occurred during the later half of glacial stage 6, consistent with the hypothesis that the Subarctic front was in a more southerly position during stage 6 than during the last glacial, and that Stage 6 was thus a more intense glacial than stage 2 (Thompson and Shackleton, 1980). The influence of the colder and more productive Subarctic waters over Shatsky Rise would thus have been more important during stage 6.

Biogenic opal constitutes 1.57 to 7.69 wt.% (mean value: 5.05%) of the sediments (Kawahata et al., 1999), with higher concentrations in the middle part of stage 8, the later part of stage 7 to the initial part of stage 6, and stage 2 to the initial part of

stage 1 (Fig. 3). There is thus no clear difference between glacial and interglacial values. Biogenic opal wt.% is influenced by the dilution by other sedimentary components, and the wt.% data were thus transformed to MAR. The MAR of biogenic opal (MAR_{opal}) exhibits a different pattern from the wt.% data, because of the relatively higher MARsediment in glacial stages. MAR_{opal} ranges between 15 and 98 mg cm^{-2} kyr^{-1} (Fig. 3), with high values in stages 6, 4, and 2 and the middle part of stage 8. The MAR_{opal} was thus in general higher during glacial stages, but there is only a weak correlation ($r = 0.67$) with the MAR of C_{org} (Fig. 3). The peaks of MAR_{opal} in stages 6, 4, and 2 correspond to those of C_{org}, but the peaks of both proxies in stage 8 do not agree. The decoupling of these two productivity proxies during stage 8 is difficult to explain, but also occurs in other data sets, e.g., in the data for the Ontong Java Plateau (Berger et al., 1994). Winnowing by removal of easily re-suspended diatoms from sediments, variations in the use of organic matter by bacteria and protists after deposition to the sea floor, or dissolution of biogenic opal might the cause of such a discrepancy, as well as variations in the part of primary produced matter contributed by diatoms.

3.3. Faunal records

The absolute abundance of benthic foraminifera (BF, number per gram of sediment) fluctuates between 291 and 3519, with an average value of 1279 (Fig. 3). The highest values occurred in glacial stages 4 and 6, a lesser peak in glacial 8, and no particularly high value in glacial stage 2. Benthic foraminiferal accumulation rates vary between 191 and 3835 (average 1217). Both the MARsediment and the absolute abundance tend to be higher during glacials, resulting in higher BFAR values during all glacials, with peak values >3000 in glacial stage 4 and the latter part of glacial stage 6. Values above 1500 occurred in all glacials.

Fifteen species occur at a relative abundance of at least 5% in at least one sample (Fig. 4), and 48 species at a relative abundance of >1% in at least one sample (Table 2). The relative abundances of the dominant species show large fluctuations (Fig. 4). The most abundant species throughout the core is *Epistominella exigua*, which occurs in all samples, at highly fluctuating abundances between 2 and 71%. *E. exigua* has peaks in glacial stages 4, 6 and 8, and in interglacial stages 5 and 7. Next in relative abundance are *Alabaminella weddellensis* and *Uvigerina peregrina*, both of which are present in all samples, at fluctuating abundances up to about 40%. There are evident problems in interpreting relative abundances of species when samples are so strongly dominated by such a small number of species, as a result of the 'fixed sum' problem.

The relative abundances of *A. weddellensis* and *E exigua*, both of which have been described as species exploiting phytodetritus (e.g., Gooday, 1993), are not positively correlated. Such a lack of positive correlation between the relative abundances of these taxa has also been described by Yasuda (1997) for the Late Miocene through Recent western equatorial Atlantic, by Loubere (1998) for the Indian Ocean, and can be seen in figures of Thomas et al. (1995) for the last 40 kyr in the northern Atlantic. There is not much knowledge about differing environmental preferences between these two species in recent environments (e.g., Gooday and Turley, 1990; Gooday et al., 1992, 1998; Gooday, 1993, 1994, 1996). King et al. (1998), however, demonstrated that *A. weddellensis* was more common than *E. exigua* in dense, laminated diatom mats in the Neogene equatorial Pacific. The abundance of these two opportunistic species might thus fluctuate, depending upon the type of phytodetritus deposited to the sea floor.

A. weddellensis had its highest peaks at 20–35 kyr (close to the boundary between glacial stage 2 and interglacial stage 3), at 170–185 kyr (in the lower part of glacial stage 6), and at 287– 298 kyr (in the lower part of glacial stage 8). These peak abundances thus appear to be close to transitions from an interglacial into a glacial period. The less common species *Eponides tenerus* (maximum relative abundance 7%) appears to have abundance fluctuations similar to those of *A. weddellensis*.

In contrast, *U. peregrina* exhibits peak values at transitions from glacial into interglacial intervals, specifically at the beginning of the present interglacial at the end of glacial stage 2, at the end of glacial stage 6, and at the end of glacial stage 8 and the beginning of interglacial stage 7. These peaks thus appear to occur at a periodicity of 100 kyr.

Of the less common species, *Bolivina translucens*

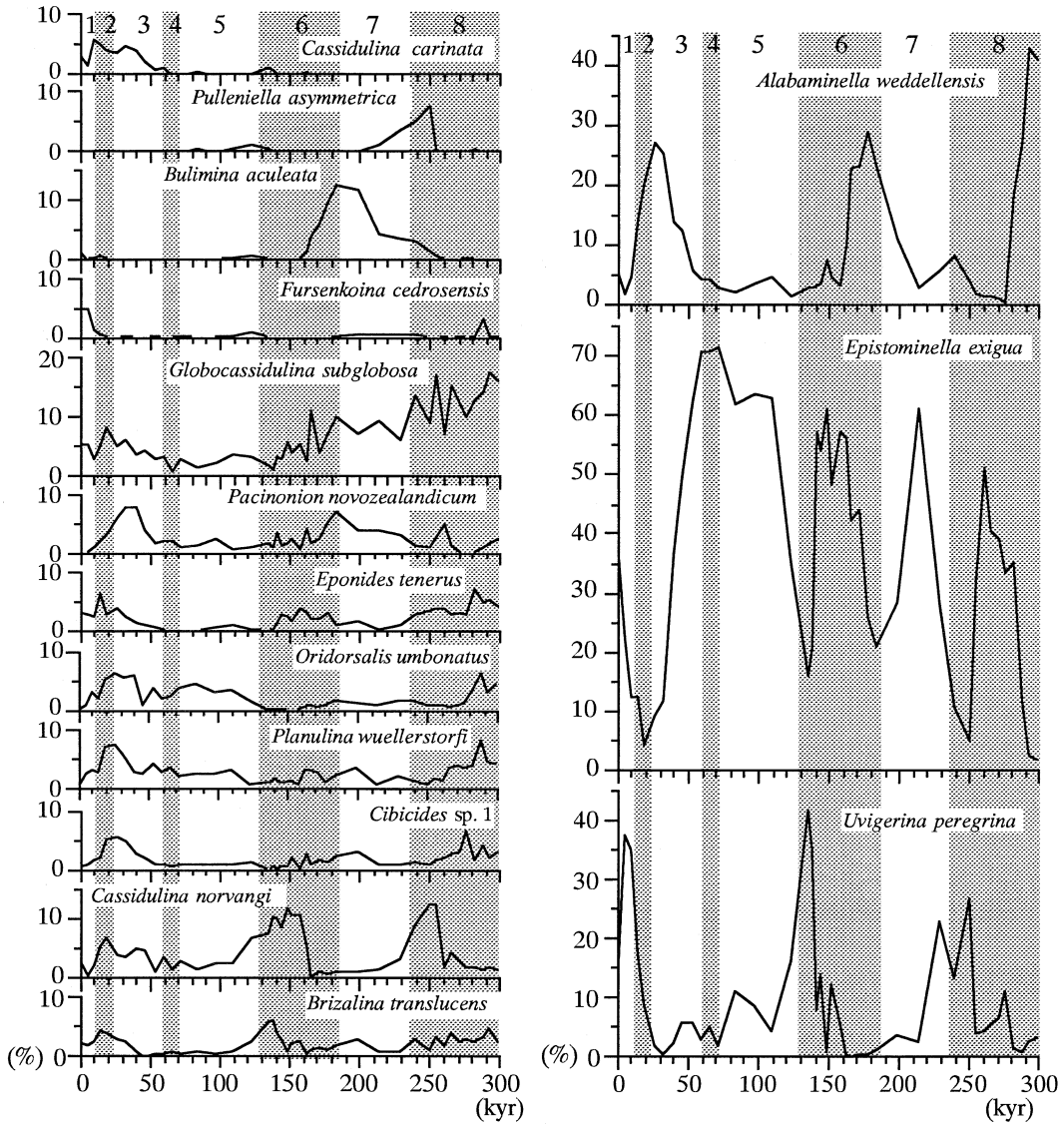

Fig. 4. Time series plots of benthic foraminiferal taxa with relative abundances >5% in at least one sample in core NGC102.

and *Cassidulina norvangi* have maximum values up to 20%, generally have high relative abundances during glacial stages, and show a distribution similar to that of *U. peregrina*. *Cibicides* sp. 1, *Oridorsalis umbonatus*, *Pacinonion novozealandicum*, and *Planulina wuellerstorfi* co-vary, and generally show higher relative abundances in stages 3 to 2, late in stage 7, and early in stage 8. *O. umbonatus* is a long-lived and cosmopolitan species, and its environmental preferences are not very clear; it lives epifaunally to shallow infaunally, and survives in food-limited, low-oxygen environments in the Sulu Sea (Rathburn and Corliss, 1994). Mackensen et al. (1995) suggested that the species reflects fairly high productivity, but well oxygenated pore waters. *Planulina wuellerstorfi* is in the northern Atlantic commonly linked to the well oxygenated North Atlantic Deep Water (NADW; e.g., Schnitker, 1974), but more recently it has been observed to live attached to objects sticking out above the sediment–

water interface, and to feed by collecting material from the water column as a suspension feeder (Lutze and Thiel, 1989). High abundance of this species has been linked to the occurrence of active bottom currents (e.g., Schnitker, 1994).

The highest relative abundance of *Bulimina aculeata* (up to 7.5%) occurred at the boundary between interglacial stage 7 and glacial stage 6. *Pulleniella asymmetrica* has its peak relative abundance (12.5%) in the later part of glacial stage 8 and into interglacial stage 7. *Cassidulina carinata* (up to 5%) is restricted to stages 1–3. *Globocassidulina subglobosa* has its highest relative abundance (up to 17%) during glacial stage 8, then generally declined in abundance to the top of the core, with the exception of a smaller peak (8.5%) in glacial stage 2. Species of *Bulimina*, *Cassidulina* and *Globocassidulina* have generally been linked to fairly high, continuous food supply (e.g., Mackensen et al., 1993, 1995; Schmiedl and Mackensen, 1997).

Q-mode factor analysis identified three dominant factors, which accounted for 92.5% of the total variance (Fig. 5; Tables 2 and 3). These three factors are mainly explained by the three most abundant species. Factor 1 comprises 70.0% of total variance, and reflects the relative abundance of *E. exigua* with a high score of 6.7. This factor thus shows high loadings in intervals where this species is most abundant (Fig. 5). Factor 2 accounts for 14.3% of the total variance, is dominantly linked to the relative abundance of *A. weddellensis*, with a highest score of 6.1, and shows high loadings where this species is abundant. Factor 3 explains 10.9% of the total variance, and dominantly reflects the relative abundance of *U. peregrina* with a high score of 6.4. High loadings of this factor thus occur at transitions from glacial to interglacial intervals and at transitions from interglacial to glacial intervals. The most important faunal changes result from the changes in relative abundances of these three abundant species.

The species diversity index varies from 13 to 29 species per 100 specimens, with an average value of 20 (Fig. 6). Peak values in diversity occur at the beginning of interglacial stages 7, 5 and 1 (but not 3), with a smaller peak at the end of interglacial stage 7. Samples with the most abundant *E. exigua* show the lowest diversity (Figs. 6 and 7), as also observed in recent faunas by Gooday et al. (1998) and Gooday

Table 3
Factor scores of the first three factors from the Q-mode varimax factor analysis of the benthic foraminiferal relative abundance data of core NGC102

Species	Factor 1	Factor 2	Factor 3
Alabaminella weddelensis	−0.59	6.14	−0.15
Brizalina translucens	−0.18	0.20	0.34
Bulimina aculeata	−0.25	−0.34	0.18
Bulimina striata	−0.17	−0.37	−0.17
Cassidulina carinata	−0.27	0.05	0.06
Cassidulina norvangi	0.01	0.09	1.18
Chilostomella oolina	−0.16	−0.37	−0.17
Cibicides sp. 1	−0.10	0.43	−0.15
Cibicidoides bradyi	−0.13	−0.39	−0.31
Cibicidoides cicatricosus	−0.10	−0.37	−0.35
Cibicidoides mundulus	−0.12	−0.36	−0.34
Epistominella exigua	6.72	0.29	0.62
Eponides lamarckianus	−0.09	−0.25	−0.33
Eponides sp. 1	−0.13	−0.29	−0.18
Eponides tenerus	−0.14	0.45	0.12
Evolvocassidulina brevis	−0.10	−0.36	−0.33
Evolvocassidulina tenuis	−0.12	−0.34	−0.34
Favocassidulina favus	−0.13	−0.38	−0.33
Fissurina abyssicola	−0.14	−0.34	−0.36
Fissurina sp. 1	−0.11	−0.37	−0.32
Francesita advena	−0.03	−0.20	−0.28
Fursenkoina cedrosensis	−0.14	−0.30	−0.13
Globocassidulina subglobosa	0.08	1.90	0.66
Gyroidina kawagatai	−0.14	−0.30	−0.20
Gyroidina sp. 1	−0.13	−0.32	−0.34
Ioanella tumidula	−0.11	−0.31	−0.28
Lagena sp.	−0.12	−0.38	−0.36
Lagenammina atlantica	−0.13	−0.38	−0.35
Melonis barleeanum	−0.19	0.04	−0.08
Melonis sphaeroides	−0.14	−0.35	−0.27
Oolina globosa	−0.14	−0.35	−0.31
Oridorsalis umbonatus	−0.14	0.57	−0.18
Pacinonion novozealandicum	0.02	0.53	−0.32
Parafissurina lateralis	−0.11	−0.36	−0.36
Planulina wuellerstorfi	−0.10	0.76	−0.13
Pullenia bolloides	−0.07	−0.39	−0.11
Pullenia okinawaensis	−0.12	−0.32	−0.29
Pullenia quinqueloba	−0.04	−0.18	−0.30
Pulleniella asymmetrica	0.02	0.18	−0.40
Pyrgo murrhina	−0.13	−0.38	−0.33
Pyrgo oblonga	−0.15	−0.38	−0.19
Quadrimorphina laevigata	−0.23	−0.37	0.27
Reophax cf. *guttifer*	−0.13	−0.38	−0.35
Stainforthia complanata	−0.06	−0.22	−0.09
Stainforthia spp.	−0.25	−0.13	0.13
Triloculina frigida	−0.10	−0.32	−0.28
Uvigerina peregrina	−0.80	−0.46	6.45
Valvulineria cf. *minuta*	−0.15	−0.34	−0.25

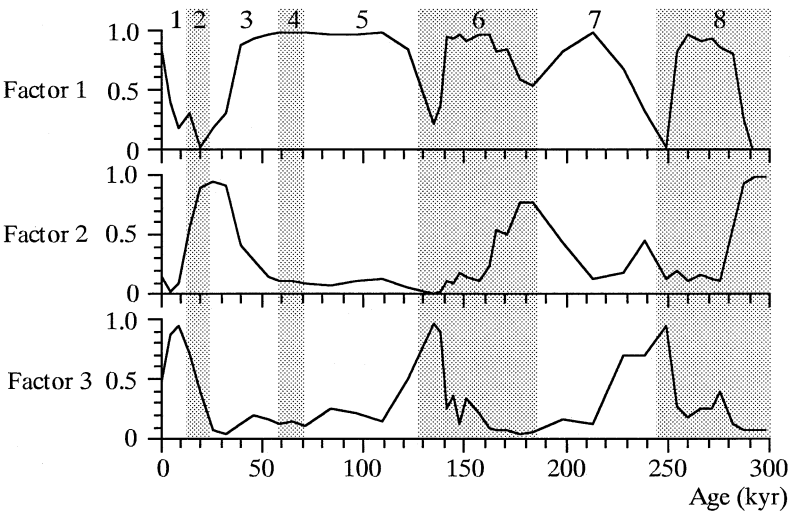

Fig. 5. Time series plots of factor loadings of the first three factors extracted based on Q-mode factor analysis of the benthic foraminiferal relative abundance data in core NGC102.

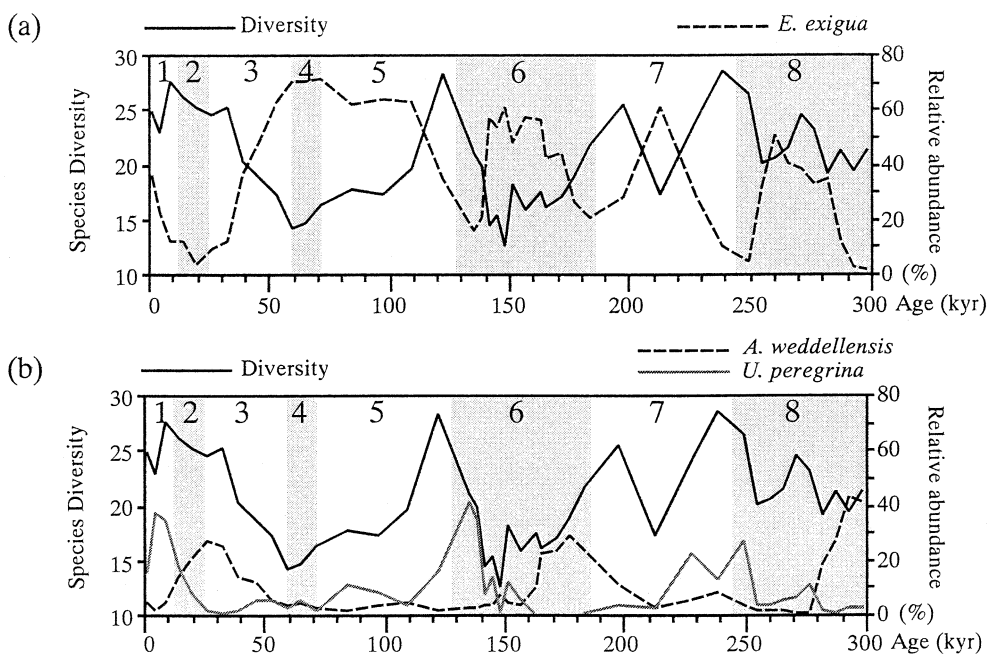

Fig. 6. (a) Comparison of the species diversity (Hurlbert's diversity index) of benthic foraminifera and the relative abundance of *Epistominella exigua*. (b) Comparison of the species diversity (Hurlbert's index) of benthic foraminifera with the relative abundance of *Alabaminella weddellensis* and *Uvigerina peregrina*.

(1999). The peak abundance of *U. peregrina* occurs in samples with a high diversity. There is no correlation between diversity and the relative abundance of *A. weddellensis*.

4. Discussion

Before we discuss the benthic foraminiferal faunal changes, we will attempt to reconstruct changes

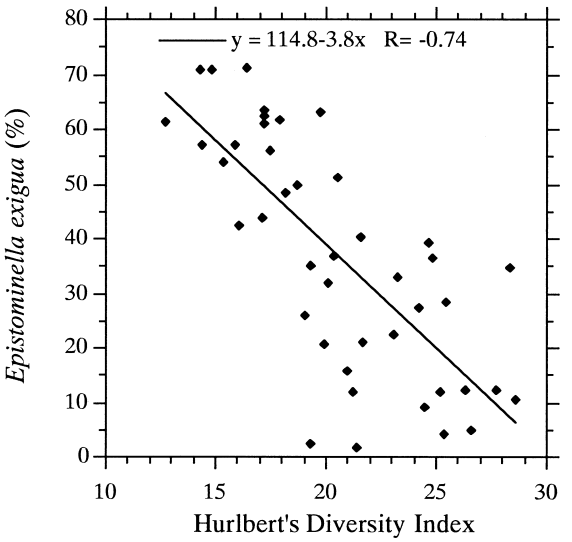

Fig. 7. Comparison of the relative abundance of *Epistominella exigua* and Hurlbert's diversity index in core NGC102.

in paleoproductivity over Shatsky Rise over the last 298 kyr. Data on C_{org} and biogenic opal of core NGC102 indicate that productivity was high in the later half of glacial stages 8 and 6, and glacial stages 4 and 2 (Fig. 3; Kawahata et al., 1999). These authors suggest that the mean organic carbon/total nitrogen atomic ratio during glacial stages (approximately 7.2) indicates that the organic matter in the sediments is mainly of marine origin (Redfield et al., 1963). Enhanced glacial productivity during the last 200 kyr occurred on Hess Rise, 20° to the east of Shatsky Rise (Kawahata et al., 1997). At northwestern Pacific middle latitudes, productivity was thus in general higher during glacial stages, and the estimated primary productivity for core NGC102 using data on C_{org} wt.% (Sarnthein et al., 1988) was approximately 70 mg cm^{-2} yr^{-1} in the late part of stages 6 and 2, compared to interglacial values of about 40 mg cm^{-2} yr^{-1} (Kawahata et al., 1999).

Glacial–interglacial re-organization of the surface current system appears to be the most plausible mechanism to explain the observed changes in productivity. The Subarctic front is presently located at about 43.5°N (Zhang and Hanawa, 1993), and moved southward to 35–38°N during stage 2, to 32–35°N during stage 6 (Thompson and Shackleton, 1980). de Silva (1999) concluded that this front did not reach the core location (32°N) during the last 298 kyr. The recent Kuroshio Extension front (KEF) occurs at 35°N and 160°E (Zhang and Hanawa, 1993; Fig. 1). If the KEF existed not only during interglacials but also during glacials, it should have moved southward together with the Subarctic front, and may have reached the coring location. Productivity would have increased if the KEF or the transition between the KEF and the Subarctic front reached the core site. The passage of such frontal systems over the core site might well have resulted in increased delivery of organic matter (including diatoms) to the core site, similar to the situation in the equatorial Pacific (e.g., Smith et al., 1996, 1997).

A second possible mechanism to explain enhanced glacial productivity would be a higher flux of aeolian dust to the region. Large quantities of alumino-silicate minerals were transported by an intensified westerly wind from Asia during the dry glacials (Hovan et al., 1991; Kawahata et al., 1997), carrying phosphorus, as well as the micronutrient iron. Such dust transport has been observed to increase productivity (e.g., Boyd et al., 1998; Cavender-Bares et al., 1999). In addition, dust transport could have assisted in the rapid transport of food particles to the sea floor (Ittekot, 1993). Both surface circulation changes and changes in nutrient supply could thus have played a role in causing higher productivity and food delivery to the sea floor during glacial intervals in the northwestern Pacific.

Benthic foraminiferal faunas give information not directly on surface productivity, but on the organic material that actually reaches the sea floor. We compared the data on the MAR of C_{org} (Kawahata et al., 1999) with the benthic foraminiferal accumulation rate (BFAR), a proxy for delivery of food to the sea floor (Herguera and Berger, 1991). BFAR may not be fully reliable as a quantitative indicator of food delivery to the sea floor because of dissolution. The temporal pattern of carbonate dissolution on Shatsky Rise is comparable to that over a wide region of the eastern equatorial Pacific, with increased dissolution during interglacials (e.g., Farrell and Prell, 1989). In order to assess possible problems in the interpretation of the benthic foraminiferal data as a result of dissolution, we compared the absolute abundance of benthic foraminifera with the dissolution index. The absolute abundance of benthic foraminifera is ex-

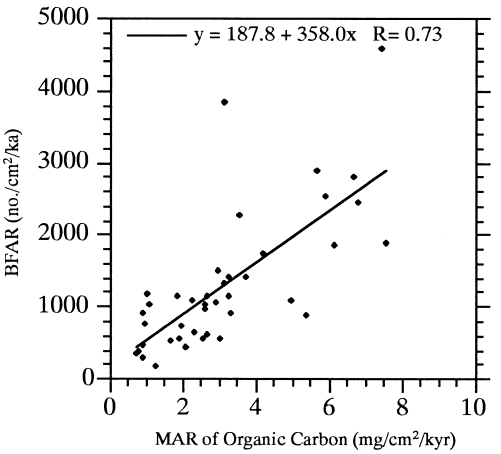

Fig. 8. Comparison of the benthic foraminiferal accumulation rate (BFAR) and the mass accumulation rate of organic carbon in core NGC102.

pected to increase as a result of dissolution of planktonic foraminifera and nannofossils. The dissolution index (Fig. 3) does not show a positive correlation with the absolute abundance of benthic foraminifera in core NGC102, suggesting that dissolution has not severely affected the benthic foraminifera.

There is a correlation ($r = 0.73$) between BFAR and MAR of C_{org} (Fig. 8), suggesting that both may indeed reflect part of the signal of food delivery to the sea floor. The correlation is not perfect, however, specifically because of the occurrence of a high peak in MAR of C_{org} in stage 2 which is not matched by a peak in BFAR, and a peak in BFAR in stage 4 which is not matched by a peak in MAR of C_{org}. The stage 4 peak in BFAR is caused by the very high abundance of *E. exigua* (a minute species indicative of pulsed phytodetritus deposition; Fig. 9), and the high numbers of specimens of this species thus may not translate into a very high foraminiferal biomass. Species composition thus may be of importance in the interpretation of benthic foraminiferal data if the smaller size fraction is used (>75 μm) instead of the fraction >150 μm as was done by Herguera and Berger (1991) and Herguera (1992). The larger size fraction contains very few of the opportunistic, phytodetritus using species, so that effects of their abundance are absent in BFAR data for that size fraction.

The species diversity is negatively correlated ($r = -0.74$) to the relative abundance of *E. exigua* (Fig. 7), and the abundance of this opportunistic species thus largely defines the diversity trends, in agreement with Gooday (1988, 1999), Thomas et al. (1995), and Thomas and Gooday (1996), who observed lower diversity faunas at higher abundances of *E. exigua*. The very high abundance of the opportunistic bloom species results in low-diversity faunas. There is no clear correlation ($r = 0.37$) between the MAR of C_{org} and the accumulation rate of *E. exigua*. Such a correlation has likewise not been observed in the northern Atlantic (Thomas et al., 1995). During the short, seasonal pulses of phytodetritus delivery to the sea floor the very reactive organic matter is commonly fully used by foraminifera and oxidized by bacteria, thus not resulting in enhanced C_{org} in the sediments (Thomas and Gooday, 1996).

Peak values of *U. peregrina* at the end of glacial stages in core NGC102 appear to be linked to high C_{org} values (Fig. 9). Many researchers have likewise reported that *U. peregrina* is linked to a high, continuous food supply in the present oceans (e.g., Lutze and Coulbourn, 1984; Mackensen et al., 1993; Rathburn and Corliss, 1994). During the end of glacial stages the coring locations thus were characterized by year-round, high deposition rates of organic material (as opposed to pulsed events), as indicated by the peak abundance of *U. peregrina*.

Peak accumulation of *E. exigua* occurred in stage 4 and the middle part of stages 8 and 6, whereas the peak accumulation of *A. weddellensis* occurred in the early parts of stages 8 and 6 and the late part of stage 3 (Fig. 9). Samples dominated by one of these species (*E. exigua* and *A. weddellensis*) should reflect lower overall food supply than samples dominated by *U. peregrina* (Smart et al., 1994; Mackensen et al., 1995; Loubere, 1998), and a pulsed, seasonal delivery of food (e.g., Gooday, 1988, 1993, 1994).

The relative abundance of *E. exigua* was high in interglacial as well as glacial stages (Fig. 4), although its accumulation rate was higher during glacials (Fig. 9). C_{org} and biogenic opal accumulation rates both indicate low productivity throughout interglacials (Fig. 9). In addition, the spring bloom results in a pulse of phytodetritus delivery, but not in year-round high deposition of phytodetritus in the recent Kuroshio Extension area. This is consistent with the interpretation that the high abundances of *E. exigua* reflects a more seasonal pattern of organic matter delivery.

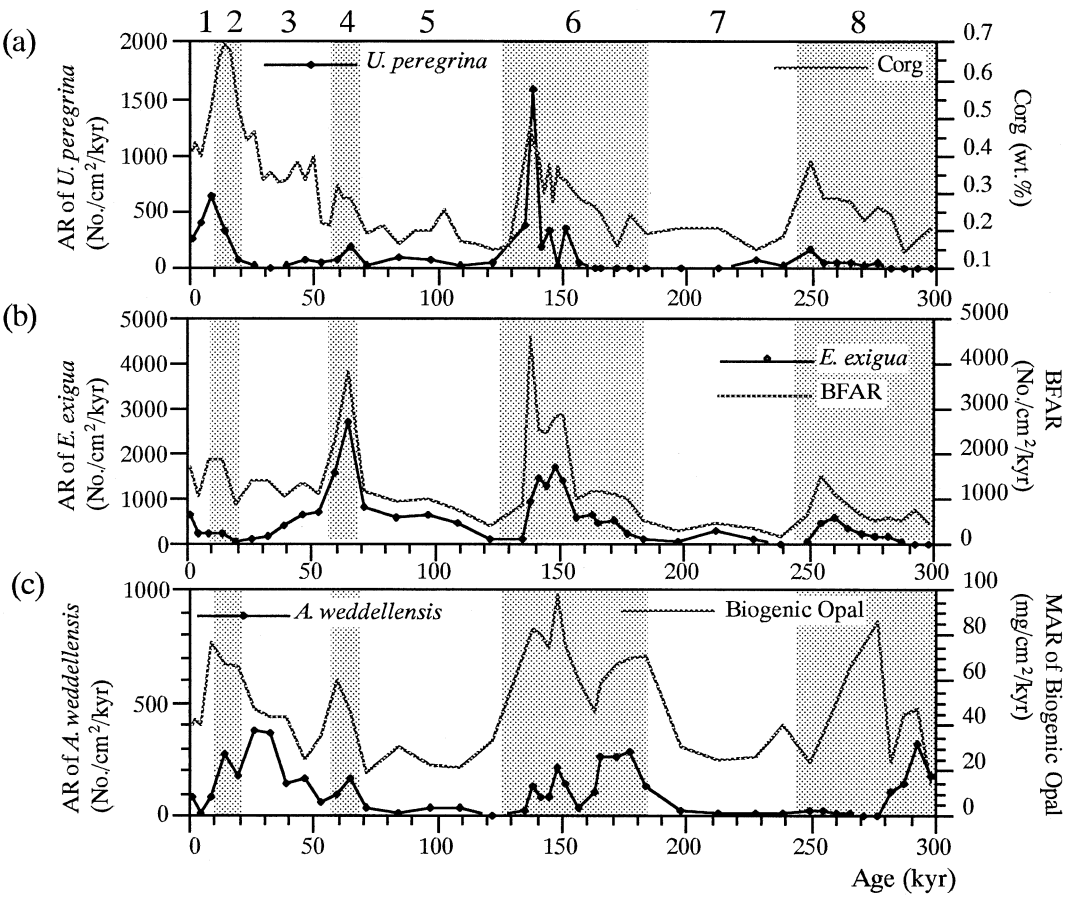

Fig. 9. (a) Comparison of the accumulation rate (AR) of *Uvigerina peregrina* and the organic carbon (C_{org}) content in core NGC102. (b) Comparison of the AR of *Epistominella exigua* and the mass accumulation rate of organic carbon in core NGC102. (c) Comparison of the AR of *Alabaminella weddellensis* and the mass accumulation rate of biogenic opal in core NGC102.

The time series plot of the accumulation rates for *A. weddellensis*, however, exhibits a different pattern than that of *E. exigua* (Fig. 9), and *E. exigua* shows a close relationship with species diversity while *A. weddellensis* does not (Fig. 6). The three peak values of both relative abundance and accumulation rate of *A. weddellensis* are restricted to glacials. This would imply that these species have different environmental preferences, and that the species reflect different ways of such a pulsed supply (Thomas et al., 1995; Yasuda, 1997; King et al., 1998). Fariduddin and Loubere (1997) reported that in the equatorial Atlantic *A. weddellensis* occurs abundantly at higher productivity than *E. exigua*. Possibly, *A. weddellensis* is more common during deposition of phytodetritus with a high proportion of needle-shaped diatoms (King et al., 1998), such as deposited below frontal zones in the equatorial Pacific (Smith et al., 1996, 1997); there is at least a slight resemblance between the time series plots of the MAR of *A. weddellensis* and MAR_{opal} (Fig. 9).

In summary, we suggest that *U. peregrina* is linked to year-round high productivity in Shatsky Rise in the last 298 kyr, and that the abundances of *E. exigua* and *A. weddellensis* are linked not just to the total delivery of organic matter, but to rapid, seasonal short-term delivery of very fresh, easily degraded organic matter. The productivity history of the last 298 kyr over Shatsky Rise thus shows strong variations in seasonality. Possibly, the strongly enhanced produc-

tivity year-round, resulting in increased deposition of organic matter to the sea floor and peak abundances of *U. peregrina*, was caused by the strongly increased dust influx (carrying nutrients) during the very dry period on the Asian continent towards the end of glacial periods, whereas the seasonally fluctuating productivity indicated during the high abundances of the 'phytodetritus species' was caused by the passage of frontal systems over Shatsky Rise, when surface circulation changed in response to a southward motion of the Subarctic front during glacial periods.

5. Conclusions

(1) The benthic foraminiferal record in a gravity core from Shatsky Rise shows large fluctuations in benthic foraminiferal accumulation rates, species composition and diversity over the last 298 kyr. The largest fluctuations resulted from variations in relative abundance of the three most abundant species *Epistominella exigua*, *Alabaminella weddellensis* and *Uvigerina peregrina*, and are probably caused by variations in productivity and its seasonality.

(2) Species diversity is negatively correlated with the relative abundances of *E. exigua* but not with that of *A. weddellensis*. This clearly reflects the opportunistic nature of *E. exigua*, but implies that these two species, both of which have been seen to respond to phytodetrital deposition in the present oceans, have different environmental preferences, possibly preferences for different types of phytodetrital material.

(3) *U. peregrina* shows peak accumulation rates at the end of glacial stages, at a periodicity of about 100 kyr, which correspond approximately to peak values in the mass accumulation rate of organic carbon. We conclude that year-round, high productivity caused these peak abundances, and occurred over Shatsky Rise during the ending phases of glacial periods, possibly as a result of increased aeolian dust influx from the Asian continent.

(4) Peak accumulation rates of *E. exigua* occurred in stage 4 and the middle part of stages 8 and 6 (but also during interglacials 5 and 7), while the peak accumulation of *A. weddellensis* occurred in the early part of stages 8 and 6 and the late part of stage 3. We suggest that high abundances of *E. exigua* and *A. weddellensis* resulted from seasonal blooms in productivity, which resulted in rapid, pulsed delivery of very fresh, easily degraded organic matter. The blooms might have resulted from passage of frontal systems over Shatsky Rise, caused by the southward motion of the Subarctic front during glacial times, even when the front itself did not reach the coring location.

Acknowledgements

We thank Kenshiro Ogasawara for his many suggestions which led to the improvement of the manuscript and Hiroshi Ujiié for his guidance in the foraminiferal identification and oxygen isotope analysis. We thank Hiro'o Natori, Akira Nishimura, Leopoldo P. de Silva Jr., Yuichiro Tanaka, Tomonori Ono, Shuntaro Oka, Kazuya Nakayama, Shungo Kawagata, Nobuhisa Eguchi, Atsushi Suzuki, Yasufusa Hatakeyama, Takashi Okamoto, Noboru Ioka, Naokazu Ahagon and Shiho Fujiwara for their help during the various phases of this study. The samples used in this study were collected during cruise NH95-2 of the Northwest Pacific Carbon Cycle Study (NOPACCS) project consigned to the Kansai Environmental Engineering Center Co. Ltd. by the New Energy and Industrial Technology Development Organization (NEDO). This work was partly supported by a Sasakawa Scientific Research Grant from the Japan Science Society. E. Thomas thanks the Geological Society of America for the 1996 Storrs Cole Award.

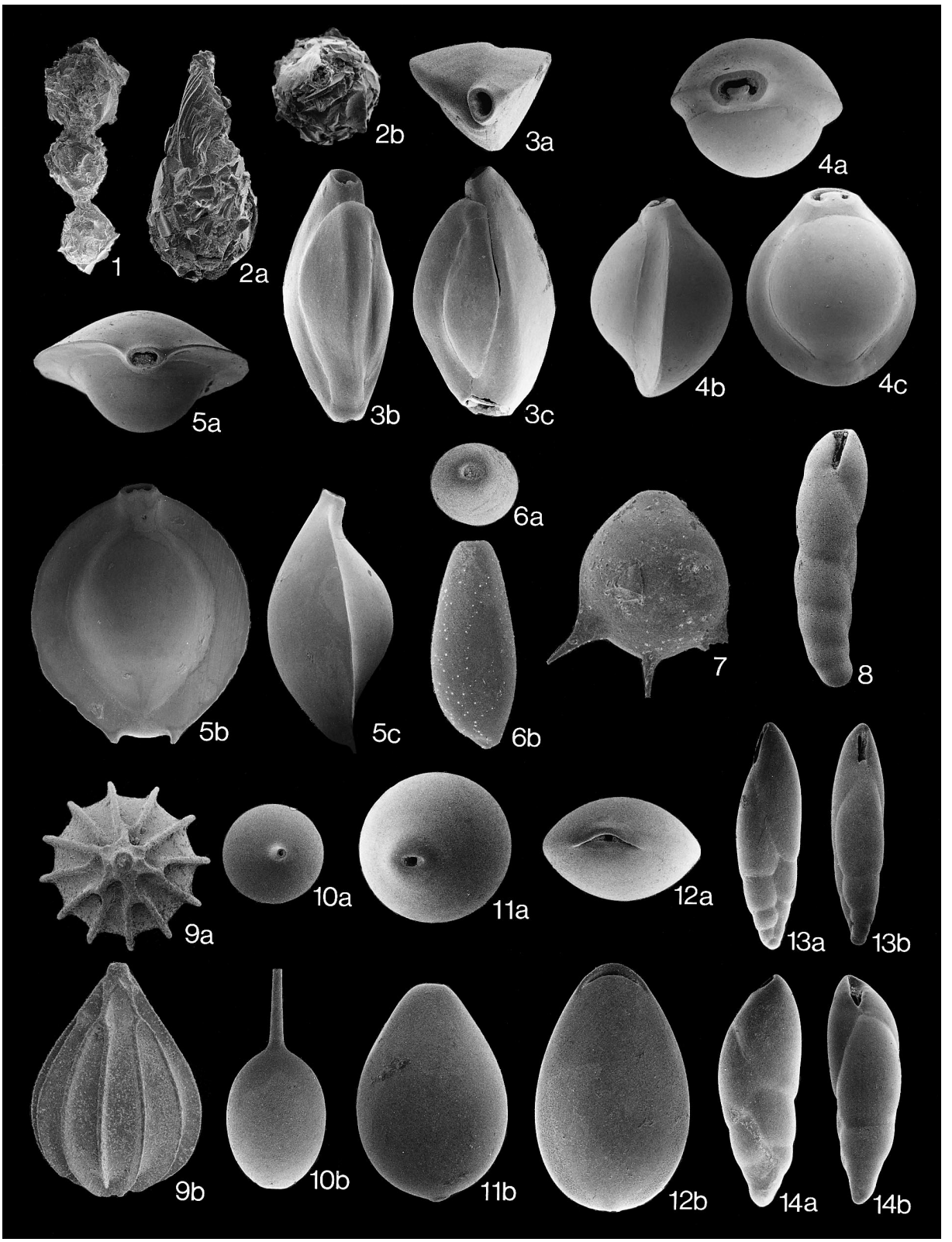
1
2a
2b
3a
4a
3b
3c
4b
4c
5a
6a
5b
5c
6b
7
8
9a
10a
11a
12a
13a
13b
9b
10b
11b
12b
14a
14b

Appendix A. Faunal references

Dominant and characteristic species in the core NGC102 from Shatsky Rise are listed alphabetically with references used for identification (Plates 1–5).

Abditodentrix pseudothalmanni = *Bolivinita pseudothalmanni* Boltovskoy and Giussani de Kahn, 1981, pp. 44–46, pl. 1, figs. 1–5.

Alabaminella weddellensis — Resig and Cheong, 1997, pl. 2, figs. 1–6.

Brizalina translucens = *Bolivina translucens* Phleger and Parker, 1951, p. 15, pl. 7, figs. 13, 14.

Bulimina aculeata — Burgess and Schnitker, 1990 fig. 2.

Bulimina striata — Ujiié, 1990, p. 31, pl. 12, figs. 9, 10.

Cassidulina carinata — Nomura, 1983, pp. 51–53, pl. 4, figs. 9–11.

Cassidulina norvangi — Nomura, 1983, pp. 53–55, pl. 4, figs. 12, 13.

Chilostomella oolina — Hermelin, 1989, p. 76, pl. 14, fig. 5.

Cibicidoides bradyi — van Morkhoven et al., 1986, pp. 100–102, pl. 30.

Cibicidoides cicatricosus — Lohmann, 1978, p. 29, pl. 2, figs. 10–12; Mead, 1985, pp. 240–242, pl. 3, 5.

Cibicidoides mundulus — van Morkhoven et al., 1986, pp. 65–67, pl. 21, fig. 1.

Epistominella exigua — Corliss, 1979, p. 7, pl. 2, figs. 7–9.

Eponides lamarckianus — Ujiié, 1990, p. 35, pl. 16, figs. 7, 8.

Plate 1

1 *Reophax* cf. *guttifer* Brady, 0–2 cm, ×200
2a, 2b *Lagenammina atlantica* (Cushman), 0–2 cm, ×250
3a–c *Triloculina frigida* Lagoe, 294–296 cm, ×250
4a–c *Pyrgo oblonga* (d'Orbigny), 139–141 cm, ×110
5a–c *Pyrgo murrhina* (Schwager), 171–173 cm, ×130
6a, 6b *Fissurina* sp. 1, 91–93 cm, ×300
7 *Fissurina abyssicola* Jones, 47–49 cm, ×400
8 *Evolvocassidulina tenuis* (Phleger and Parker), 271–273 cm, ×130
9a, 9b *Lagena* sp., 294–296 cm, ×350
10a, 10b *Lagena nebulosa* Cushman, 271–273 cm, ×200
11a, 11b *Oolina globosa* (Montagu), 23–25 cm, ×250
12a, 12b *Parafissurina lateralis* (Cushman), 63–65 cm, ×250
13a, 13b *Stainforthia feylingi* Knudsen and Seidenkrantz, 326–328 cm, ×200
14a, 14b *Stainforthia* sp., 15–17 cm, ×200

Plate 2 (see p. 140)

1a, 1b *Cassidulina carinata* Silvestri, 15–17 cm, ×220
2 *Bulimina aculeata* d'Orbigny, 247–249 cm, ×150
3 *Bulimina striata* d'Orbigny, 139–141 cm, ×130
4 *Uvigerina peregrina* Cushman, 7–9 cm, ×110
5a, 5b *Favocassidulina favus* (Brady), 7–9 cm, ×160
6a–c *Cassidulina norvangi* Thalmann, 123–125 cm, ×250
7 *Evolvocassidulina brevis* (Aoki), 123–125 cm, ×350
8 *Globocassidulina subglobosa* (Brady), 279–281 cm, ×400
9a–c *Ioanella tumidula* (Brady), 123–125 cm, ×350
10 *Stainforthia complanata* (Egger), 131–133 cm, ×200
11a, 11b *Bolivina translucens* Phleger and Parker, megalospheric form, 310–312 cm, ×200
12a, 12b *Bolivina translucens* Phleger and Parker, microspheric form, 310–312 cm, ×200
13 *Fursenkoina cedrosensis* (McCulloch), 0–2 cm, ×250
14 *Francesita advena* (Cushman), 279–281 cm, ×200
15 *Chilostomella oolina* Schwager, 139–141 cm, ×150

Plate 3 (see p. 141)

1a, 1b, 1c *Epistominella exigua* (Brady), 179–181 cm, ×230
2a, 2b, 2c *Quadrimorphina laevigata* (Phleger and Parker), 131–133 cm, ×200
3a, 3b, 3c *Alabaminella weddellensis* (Earland), 326–328 cm, ×350
4a, 4b, 4c *Gyroidina kawagatai* (Ujiié), 279–281 cm, ×200
5a, 5b, 5c *Gyroidina* sp. 1, 310–312 cm, ×250
6a, 6b, 6c *Louisianina minuta* (Ujiié), 287–289 cm, ×450
7a, 7b, 7c *Eponides* sp. 1, 163–165 cm, ×300
8a, 8b, 8c *Eponides* sp. 1, 163–165 cm, ×300

Plate 4 (see p. 142)

1a, 1b, 1c *Planulina wuellerstorfi* (Schwager), 310–312 cm, ×130
2a, 2b, 2c *Cibicides* sp. 1, 55–57 cm, ×250
3a, 3b, 3c *Cibicidoides mundulus* (Brady, Parker and Jones), 239–241 cm, ×110
4a, 4b, 4c *Cibicidoides cicatricosus* (Schwager), 163–165 cm, ×180
5a, 5b, 5c *Eponides lamarckianus* (d'Orbigny), 55–57 cm, ×250
6a, 6b, 6c *Cibicidoides bradyi* (Trauth), 0–2 cm, ×200
7a, 7b *Pulleniella asymmetrica* Ujiié, 223–225 cm, ×200

Plate 5 (see p. 143)

1a, 1b, 1c *Oridorsalis umbonatus* (Reuss), 47–49 cm, ×130
2a, 2b *Pullenia quinqueloba* (Reuss), 131–133 cm, ×150
3a, 3b, 3c *Eponides tenerus* (Brady), 47–49 cm, ×130
4a, 4b *Pullenia okinawaensis* Ujiié, 247–249 cm, ×300
5a, 5b *Pacinonion novozealandicum* (Cushman and Edwards), 215–217 cm, ×230
6a, 6b *Melonis barleeanum* (Williamson), 39–41 cm, ×150
7a, 7b *Melonis sphaeroides* Voloshinova, 263–265 cm, ×130
8a, 8b *Valvulineria* cf.*minuta* (Schubert), 47–49 cm, ×200
9a, 9b *Pullenia bulloides* (d'Orbigny), 287–289 cm, ×150
10a, 10b *Valvulineria* cf. *minuta* (Schubert), 247–249 cm, ×200

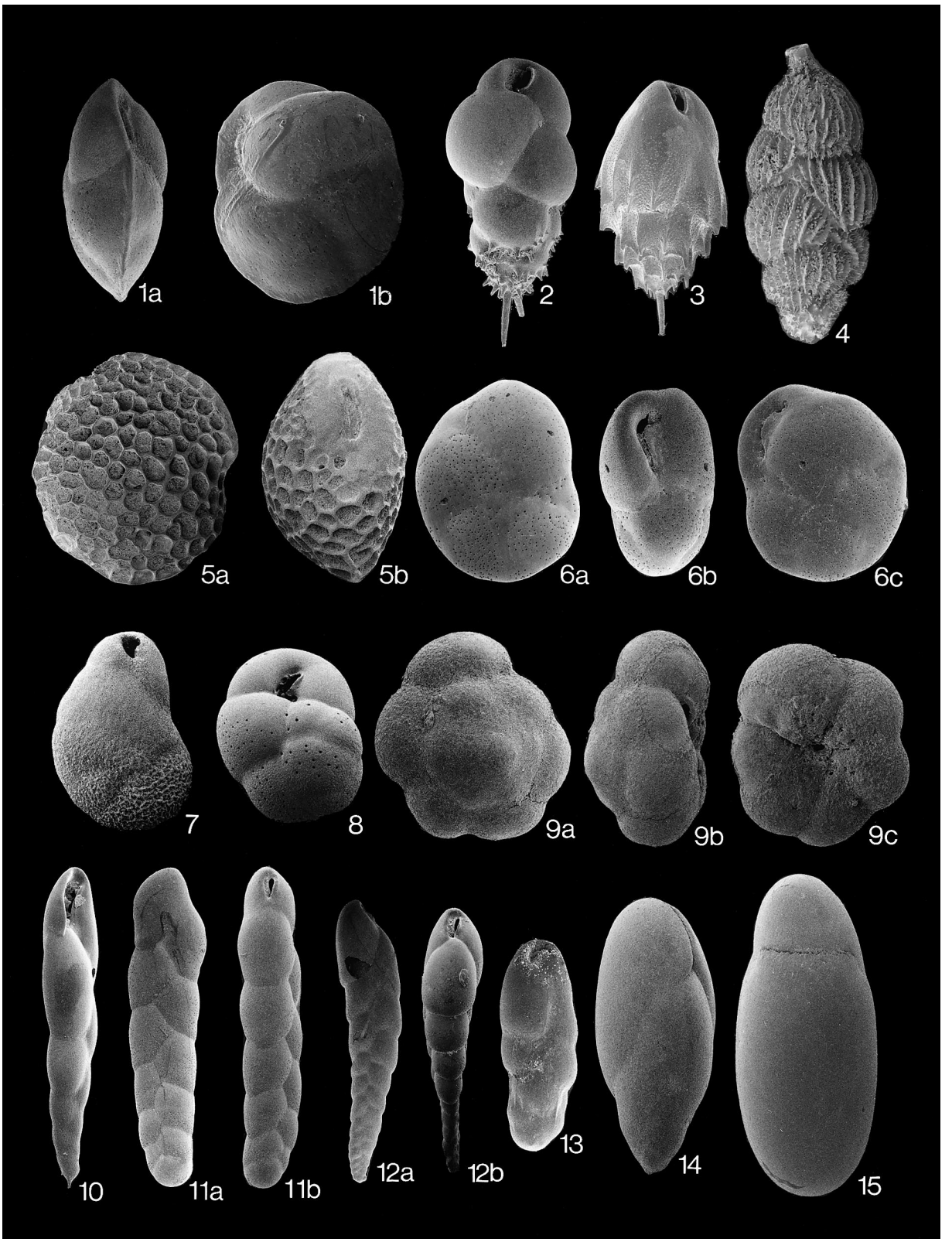
1a
1b
2
3
4
5a
5b
6a
6b
6c
7
8
9a
9b
9c
10
11a
11b
12a
12b
13
14
15

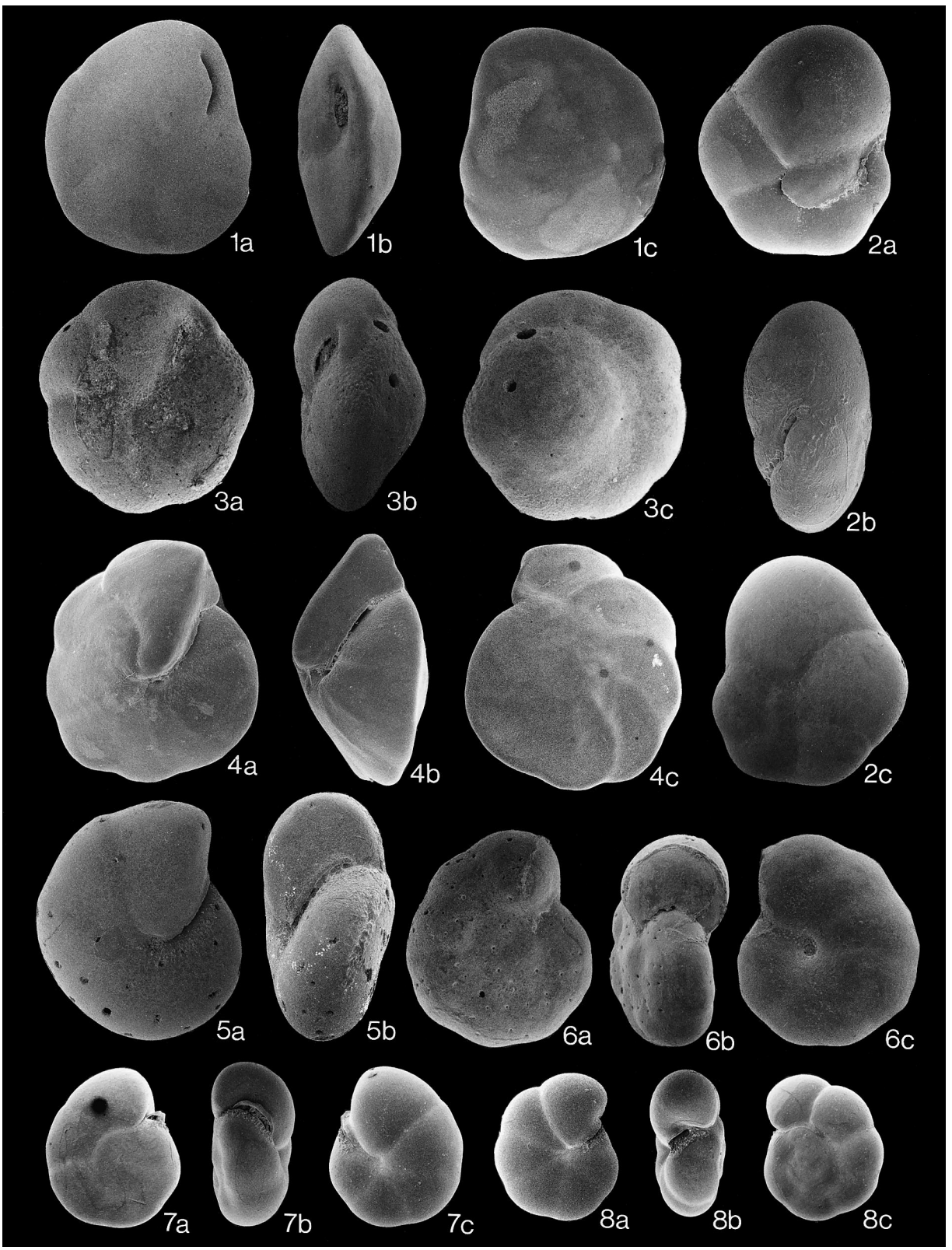
1a
1b
1c
2a
3a
3b
3c
2b
4a
4b
4c
2c
5a
5b
6a
6b
6c
7a
7b
7c
8a
8b
8c

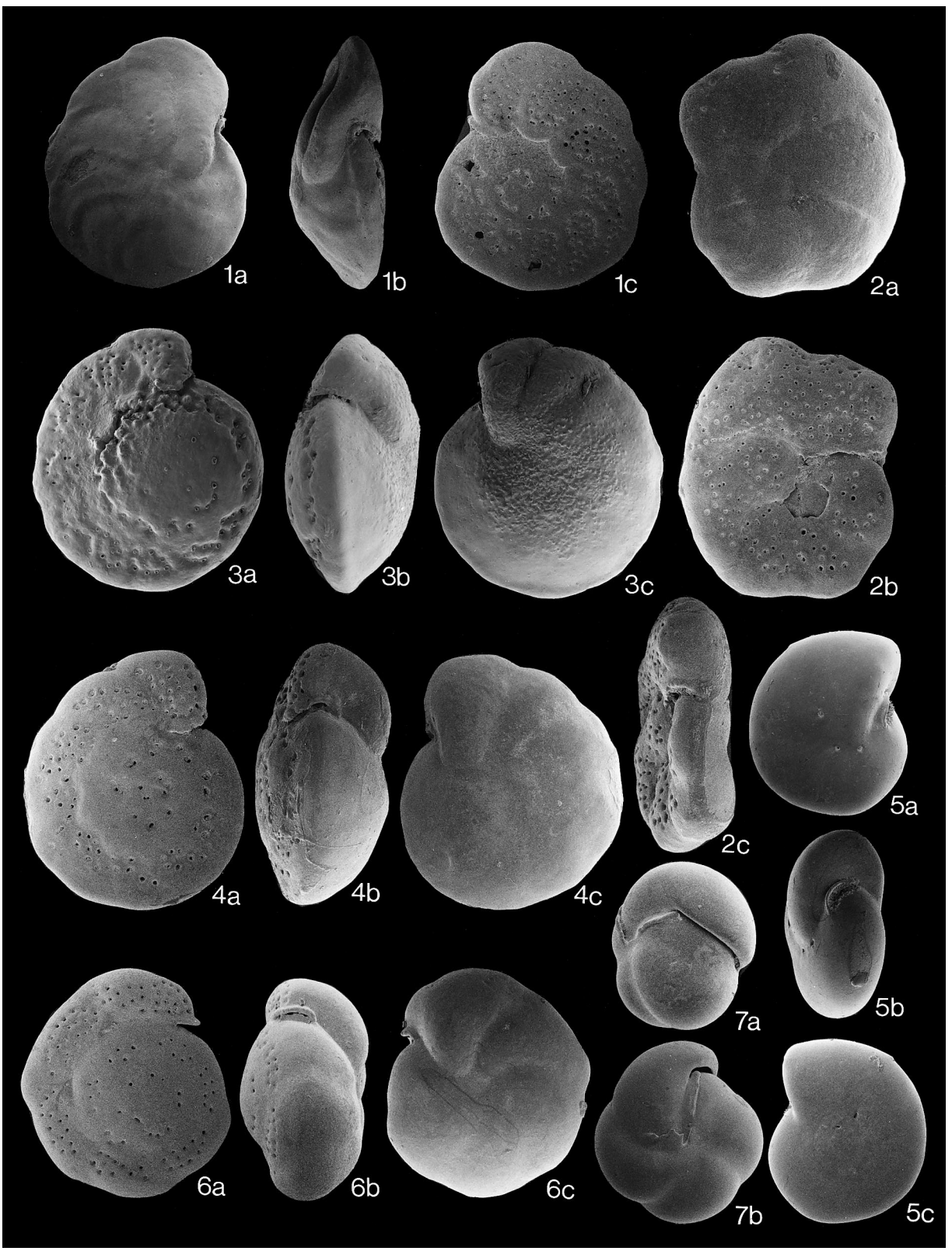
1a
1b
1c
2a
3a
3b
3c
2b
4a
4b
4c
2c
5a
7a
5b
6a
6b
6c
7b
5c

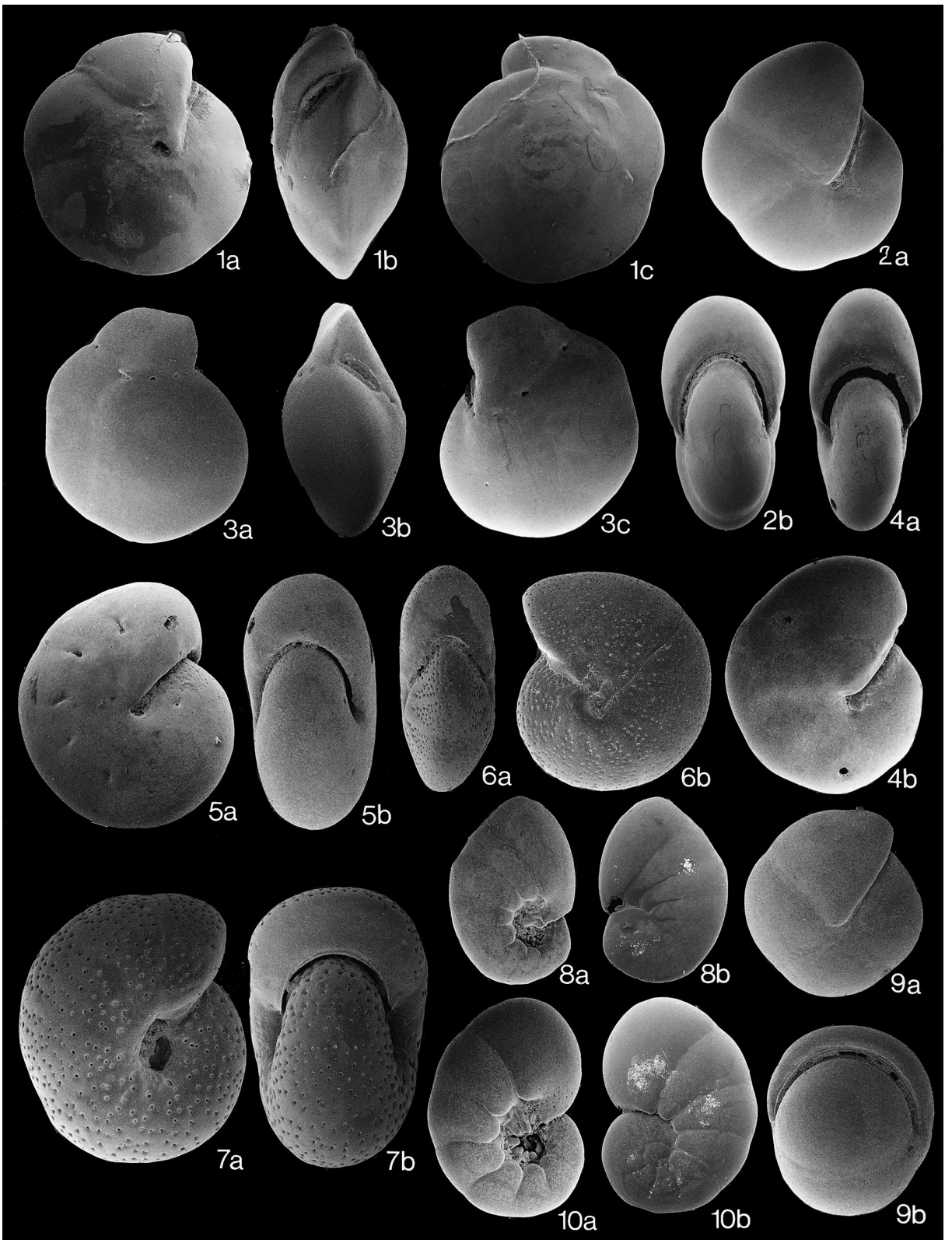
1a
1b
1c
2a
3a
3b
3c
2b
4a
5a
5b
6a
6b
4b
8a
8b
9a
7a
7b
10a
10b
9b

Eponides tenerus — Ujiié, 1990, pp. 34–35, pl. 16, figs. 5, 6.
Evolvocassidulina brevis — Nomura, 1983, p. 49, pl. 4, figs. 4–7.
Evolvocassidulina tenuis — Ujiié, 1990, p. 38, pl. 18, figs. 10–14.
Favocassidulina favus — Hermelin, 1989, p. 74, pl. 13, figs. 14, 17.
Fissurina abyssicola Jones, 1984, pp. 111–112, pl. 3, fig. 16.
Francesita advena — Boltovskoy, 1978, p. 160, pl. 4, figs. 6–8.
Fursenkoina cedrosensis — Xu and Ujiié, 1994, pl. 8, fig. 1; Ujiié, 1995, pl. 7, fig. 2.
Globocassidulina subglobosa — Belford, 1966, pp. 149–150, pl. 25, figs. 11–16.
Gyroidina kawagatai = *Gyroidinoides kawagatai* Ujiié, 1995, pl. 14, figs. 3, 4.
Ioanella tumidula — Loeblich and Tappan, 1988, pp. 549–550, pl. 595, figs. 4–10.
Lagenammina atlantica — Ujiié, 1995, p. 55, pl. 1, fig. 16.
Lagena nebulosa — Ujiié, 1990, p. 18, pl. 5, fig. 5.
Melonis barleeanum — Corliss, 1979, p. 10, 12, pl. 5, figs. 7, 8.
Melonis sphaeroides — Hasegawa, 1984, pl. 1, figs. 1–3; Whittaker, 1988, p. 165, pl. 24, figs. 28, 29.
Oolina globosa — Hermelin, 1989, p. 56, pl. 10, fig. 4.
Oridorsalis umbonatus. Ujiié, 1990, pp. 48–49, pl. 28, figs. 1–3, 5, 6.
Pacinonion novozealandicum — Vella, 1962, p. 290, pl. 1, figs. 10, 11; Ujiié, 1995, p. 69, pl. 12, fig. 1.
Parafissurina lateralis — Loeblich and Tappan, 1994, p. 94, pl. 164, figs. 1–10.
Planulina wuellerstorfi — van Morkhoven et al., 1986, pp. 48–50, pl. 14, figs. 1, 2.
Pullenia bulloides — Mead, 1985, p. 236, pl. 4, fig. 6.
Pullenia quinqueloba — Cushman and Todd, 1943, p. 11, pl. 2, fig. 8; Ujiié, 1990, pl. 24, figs. 1–5.
Pullenia okinawaensis Ujiié, 1995, p.70, pl. 12, fig. 9.
Pulleniella asymmetrica Ujiié, 1990, p. 45, pl. 23, figs. 3, 4.
Pyrgo murrhina — Boltovskoy, 1978, p. 167, pl. 6, fig. 26.
Pyrgo oblonga — Ujiié, 1990, p. 16, pl. 3, fig. 9.
Quadrimorphina laevigata — Ujiié, 1990, p. 41, pl. 15, fig. 1.
Stainforthia complanata — Resig, 1981, pl. 5, fig. 16.
Stainforthia feylingi Knudsen and Seidenkrantz, 1994, pp. 5–7, pl. 1, figs. 1–3.
Triloculina frigida Lagoe, 1977, p. 120, figs. 6, pl. 1, figs. 12, 17.
Uvigerina peregrina — Lamb and Miller, 1984, pp. 6–7, pl. 8, figs. 1–6; pl. 9, figs. 1–5.
Valvulineria cf. *minuta* = *Rotamorphina minuta*, Belford, 1966, p. 156, pl. 37, figs. 11–15; Ujiié, 1990, p. 42, pl. 15, figs. 2, 3.

References

Akimoto, K., 1990. Distribution of Recent benthic foraminiferal faunas in the Pacific off southwest Japan and around Hachijo-jima Island. Sci. Rep. Tohoku Univ., 2nd Ser. 60, 139–223.

Belford, D.J., 1966. Miocene and Pliocene smaller Foraminifera from Papua and New Guinea. Aust. Bur. Miner. Res. Geol. Geophys., Bull. 79, 1–306.

Berger, W.H., Adelseck, C.G., Mayer, L.A., 1976. Distribution of carbonate in surface sediments of the Pacific Ocean. J. Geophys. Res. 81, 2617–2627.

Berger, W.H., Herguera, J.C., Lange, C.B. and Schneider, R., 1994. Paleoproductivity: flux proxies versus nutrient proxies and other problems concerning the Quaternary productivity record. In: Zahn, R. et al. (Eds.), Carbon Cycling in the Glacial Changes. Springer, Berlin, pp. 385–412.

Boltovskoy, E., 1978. Late Cenozoic benthonic foraminifera of the Ninetyeast Ridge (Indian Ocean). Mar. Geol. 26, 139–175.

Boltovskoy, E., Giussani de Kahn, G., 1981. Cinco nuevos taxones en Orden Foraminiferida. Com. Mus. Arg. Cie. Nat. (Bernardino Rivadavia) Inst. Nac. Invest. Cie. Nat., Hydrobiol. 2, 43–51.

Boyd, P.W., Wong, C.S., Merrill, J., Whitney, F., Snow, J., Harrison, P.J., Gower, J., 1998. Atmospheric iron supply and enhanced vertical carbon flux in the NE subarctic Pacific: is there a connection? Global Biogeochem. Cycles 12, 429–441.

Burgess, M.V., Schnitker, D., 1990. Morphometry of *Bulimina aculeata* Orbigny and *Bulimina marginata* Orbigny. J. Foraminiferal Res. 20, 37–49.

Cavender-Bares, K.K., Mann, E.L., Chisholm, S., Ondrusek, M.E., Bidigare, R.R., 1999. Differential response of equatorial Pacific phytoplankton to iron fertilization. Limnol. Oceanogr. 44, 237–246.

Corliss, B.H., 1979. Taxonomy of Recent deep-sea benthonic foraminifera from the southeast Indian Ocean. Micropaleontology 25, 1–19.

Corliss, B.H., 1991. Morphology and microhabitat preferences of benthic foraminifera from the northwest Atlantic Ocean. Mar. Micropaleontol. 17, 195–236.

Corliss, B.H., Chen, C., 1988. Morphotype patterns of Norwegian deep-sea benthic foraminifera and ecological implications. Geology 16, 716–719.

Cushman, J.A., Todd, R., 1943. The genus *Pullenia* and its species. Contrib. Cushman Lab. Foraminiferal Res. 19, 1–23.

de Silva, Jr. L.P., 1999. Late Quaternary Carbonate Preservation History and Sea Surface Paleoceanography of the Shatsky Rise, Northwestern Pacific. Ph.D. Thesis, Univ. Tsukuba, Ibaraki, 151 pp.

Fariduddin, M., Loubere, P., 1997. The surface ocean productivity response of deeper water benthic foraminifera in the Atlantic Ocean. Mar. Micropaleontol. 32, 289–310.

Farrell, J.W., Prell, W.L., 1989. Climate change and $CaCO_3$ preservation: an 800,000 year bathymetric reconstruction from the central equatorial Pacific Ocean. Paleoceanography 4, 447–466.

Gage, J.D., Tyler, P.A., 1991. Deep-Sea Biology: A Natural History of Organisms at the Deep-Sea Floor. Cambridge University Press, Cambridge, 504 pp.

Gooday, A.J., 1988. A response by benthic Foraminifera to the deposition of phytodetritus in the deep sea. Nature 332, 70–73.

Gooday, A.J., 1993. Deep-sea benthic foraminiferal species

which exploit phytodetritus: characteristic features and controls on distribution. Mar. Micropaleontol. 22, 187–205.
Gooday, A.J., 1994. The biology of deep-sea foraminifera: a review of some advances and their applications in paleoceanography. Palaios 9, 14–31.
Gooday, A.J., 1996. Epifaunal and shallow infaunal foraminiferal communities at three abyssal NE Atlantic sites subject to differing phytodetritus input regimes. Deep Sea Res. I 43, 1395–1421.
Gooday, A.J., 1999. Biodiversity of Foraminifera and other protists in the deep sea: scales and patterns. Belg. J. Zool. 129, 61–80.
Gooday, A.J., Turley, C.M., 1990. Responses by benthic organisms to inputs of organic material to the ocean floor. Philos. Trans. R. Soc. London, Ser. A 331, 119–138.
Gooday, A.J., Levin, L.A., Linke, P., Heeger, T., 1992. The role of benthic foraminifera in deep-sea food webs and carbon cycling. In: Rowe, G.T., Pariente, V. (Eds.), Deep-Sea Food Chains and the Global Carbon Cycle, Kluwer, Rotterdam, pp. 63–91.
Gooday, A.J., Bett, B.J., Shires, R., Lambshead, P.J.D., 1998. Deep-sea benthic foraminiferal species diversity in the NE Atlantic and NW Arabian Sea: a synthesis. Deep Sea Res. II 45, 165–201.
Hasegawa, S., 1984. Notes on the taxonomy and paleoecology of *Melonis pompilioides* and its allied taxa from Japan. In: Oertli, H.J. (Ed.), Benthos '83; Second International Symposium on Benthic Foraminifera (Pau, April 1983). Pau and Bordeaux, pp. 299–304.
Herguera, J.C., 1992. Deep-sea benthic foraminifera and biogenic opal: glacial to postglacial productivity changes in the western equatorial Pacific. Mar. Micropaleontol. 19, 79–98.
Herguera, J.C., Berger, W.H., 1991. Paleoproductivity from benthic foraminifera abundance: Glacial to postglacial change in the west-equatorial Pacific. Geology 19, 1173–1176.
Hermelin, J.O.R., 1989. Pliocene benthic foraminifera from the Ontong-Java Plateau (western equatorial Pacific Ocean): faunas response to changing paleoenvironment. Cushman Found. Foraminiferal Res., Spec. Publ. 26, 1–143.
Hermelin, J.O.R., Shimmield, G.B., 1995. Impact of productivity events on the benthic foraminiferal fauna in the Arabian Sea over the last 150,000 years. Paleoceanography 10, 85–116.
Hovan, S.A., Rea, D.K., Pisias, N.G., 1991. Late Pleistocene continental climate and oceanic variability recorded in Northwest Pacific sediments. Paleoceanography 6, 349–370.
Hurlbert, S.H., 1971. The nonconcept of species diversity: a critique and alternative parameters. Ecology 52, 577–586.
Imbrie, J., Hays, J.D., Martinson, D.G., Mcintyre, A., Mix, A.C., Morley, J.J., Pisias, N.G., Prell, W.L., Shackleton, N.J., 1984. The orbital theory of Pleistocene climate: support from a revised chronology of the marine $\delta^{18}O$ record. In: Berger, A., Imbrie, J., Kukla, G., Saltzman, B. (Eds.), Milankovitch and Climate, Part I. Reidel, Dordrecht, pp. 269–305.
Ittekot, V., 1993. The abiotically driven biological pump in the ocean and short-term fluctuations in atmospheric CO_2 contents. Global Planet. Change 8, 17–25.
Jannink, N.T., Zachariasse, W.J., van der Zwaan, G.J., 1998. Living (Rose Bengal stained) benthic foraminifera from the Pakistan continental margin (northern Arabian Sea). Deep Sea Res. I 45, 1483–1513.
Jones, R.W., 1984. A revised classification of the unilocular Nodosariida and Buliminida (Foraminifera). Rev. Esp. Micropaleontol. 14, 91–160.
Jorissen, F.J., De Stigter, H.C., Widmark, J., 1995. A conceptual model explaining benthic foraminiferal microhabitats. Mar. Micropaleontol. 26, 3–15.
Kawagata, S., Ujiié, H., 1996. Distribution and environmental relationships of Recent bathyal foraminifera in the Ryukyu Island Arc region, northwest Pacific Ocean. J. Foraminiferal Res. 26, 342–356.
Kawahata, H., Okamoto, T., Ujiié, H., Ito, Y., Matsumoto, E., 1997. The fluctuation of the accumulation rate of aerosol in the Hess Rise, North Pacific, during the last 200 kyr: estimation of aerosol effect to carbon cycle (in Japanese with English abstract). J. Geol. Soc. Jpn. 103, 475–483.
Kawahata, H., Suzuki, A., Ohta, H., 1998. Sinking particles between the equatorial and Subarctic regions (0ºN–46ºN) in the central Pacific. Geochem. J. 32, 125–133.
Kawahata, H., Ohkushi, K., Hatakeyama, Y., 1999. Comparison of the fluctuation of biogenic sedimentation in the boreal and austral middle latitude of the western Pacific during the Late Pleistocene. J. Oceanogr. (in press).
King, S.C., Murray, J.W., Kemp, A.E.S., 1998. Palaeoenvironments of deposition of Neogene laminated diatom at deposits from the eastern equatorial Pacific from studies of benthic foraminifera (Sites 844, 849, 851). Mar. Micropaleontol. 35, 161–177.
Kitazato, H., Ohga, T., 1995. Seasonal changes in deep-sea benthic foraminiferal populations: results of long-term observations at Sagami Bay, Japan. In: Sakai, H., Nozaki, Y. (Eds.), Biogeochemical Processes and Ocean Flux in the Western Pacific, Terra Sci. Publ., Tokyo, pp. 331–342.
Knudsen, K.L., Seidenkrantz, M.-S., 1994. *Stainforthia feylingi* new species from Arctic to subarctic environments, previously recorded as *Stainforthia schreibersiana* (Czjzek). In: Sejrup, H.P., Knudsen, K.L. (Eds.), Late Cenozoic Benthic Foraminifera: Taxonomy and Stratigraphy. Cushman Found., Spec. Publ. 32, 5–13.
Lagoe, M.B., 1977. Recent benthic foraminifera from the central Arctic Ocean. J. Foraminiferal Res. 7, 106–129.
Lamb, J.L., Miller, T.L., 1984. Stratigraphic Significance of Uvigerinid Foraminifers in the Western Hemisphere. The University of Kansas Paleontological Contributions, 66, Univ. of Kansas Paleontological Institute, 100 pp.
Levine, E.R., White, W.B., 1983. Bathymetric influences upon the character of the North Pacific fronts, 1976–198. J. Geophys. Res. 88, 9617–9625.
Loeblich, A.R., Jr., Tappan, H., 1988. Foraminiferal Genera and their Classification. Van Nostrand Reinhold, New York, 970 pp.
Loeblich Jr., A.R., Tappan, H., 1994. Foraminifera of the Sahul Shelf and Timor Sea. Cushman Found. Foraminiferal Res., Spec. Publ. 31, 1–661.
Lohmann, G.P., 1978. Abyssal benthonic foraminifera as hy-

drographic indicators in the western south Atlantic Ocean. J. Foraminiferal Res. 8, 6–34.

Loubere, P., 1991. Deep-sea benthic foraminiferal assemblage response to a surface ocean productivity gradient: a test. Paleoceanography 6, 193–204.

Loubere, P., 1994. Quantitative estimation of surface ocean productivity and bottom water oxygen concentration using benthic foraminifera. Paleoceanography 9, 723–737.

Loubere, P., 1996. The surface ocean productivity and bottom water oxygen signals in deep water benthic foraminiferal assemblages. Mar. Micropaleontol. 28, 247–261.

Loubere, P., 1998. The impact of seasonality on the benthos as reflected in the assemblages of benthic foraminifera. Deep Sea Res. I 45, 409–432.

Loubere, P., Fariduddin, M., 1999. Quantitative estimation of global patterns of surface ocean biological productivity and its seasonal variation on time scales from centuries to millennia. Global Biogeochem. Cycles 13, 115–133.

Lutze, G.F., Coulbourn, W.T., 1984. Recent benthic foraminifera from the continental margin of Northwest Africa: community structure and distribution. Mar. Micropaleontol. 8, 361–401.

Lutze, G.F., Thiel, H., 1989. *Cibicidoides wuellerstorfi* and *Planulina ariminensis*, elevated epibenthic foraminifera. J. Foraminiferal Res. 19, 153–158.

Mackensen, A., Fütterer, D.K., Grobe, H., Schmiedl, G., 1993. Benthic foraminiferal assemblages from the eastern Southern Atlantic Polar Front region between 35 and 75°S: distribution, ecology and fossilization potential. Mar. Micropaleontol. 22, 33–69.

Mackensen, A., Schmiedl, G., Harloff, J., Giese, M., 1995. Deep-sea foraminifera in the South Atlantic Ocean: ecology and assemblage generation. Micropaleontology 41, 342–358.

Maiya, S., Saito, T., Sato, T., 1976. Late Cenozoic planktonic foraminiferal biostratigraphy of northwest Pacific sedimentary sequences. In: Takayanagi, Y., Saito, T. (Eds.), Progress in Micropaleontology. Micropaleontology Press, New York, pp. 395–422.

Matoba, Y., 1976. Recent foraminiferal assemblages off Sendai, northeast Japan. In: Schafer, C.T., Pelletier, B.R. (Eds.), First International Symposium on Benthonic Foraminifera of Continental Margins, Maritime Sediments, pp. 205–220.

Mead, G.A., 1985. Recent benthic foraminifera in the Polar Front region of the southwest Atlantic. Micropaleontology 31, 221–248.

Mizuno, K., White, W.B., 1983. Annual and interannual variability in the Kuroshio Current System. J. Phys. Oceanogr. 13, 1847–1867.

Nomura, R., 1983. Cassidulinidae (Foraminiferida) from the uppermost Cenozoic of Japan (Part 2). Sci. Rep. Tohoku Univ., 2nd Ser. 54, 1–93.

Ohga, T., Kitazato, H., 1997. Seasonal changes in bathyal foraminiferal populations in response to the flux of organic matter (Sagami Bay, Japan). Terra Nova 9, 33–37.

Phleger, F.B., Parker, F.L., 1951. Ecology of foraminifera, northwest Gulf of Mexico, II. Foraminifera species. Mem. Geol. Soc. America 46, 1–64.

Rathburn, A.E., Corliss, B.H., 1994. The ecology of living (stained) benthic foraminifera from the Sulu Sea. Paleoceanography 9, 87–150.

Redfield, A.C., Ketchum, B.H., Richards, F.A., 1963. The influence of organisms on the composition of sea water. In: Hill, M.N. (Ed.), The Sea. Wiley, New York, pp. 26–77.

Resig, J.M., 1981. Biogeography of benthic foraminifera of the northern Nazca Plate and adjacent continental margin. Geol. Soc. Am. Mem. 154, 619–665.

Resig, J.M., Cheong, H.-K., 1997. Pliocene–Holocene benthic foraminiferal assemblages and water mass history, ODP 806B, western equatorial Pacific. Micropaleontology 43, 419–439.

Roden, G.I., 1975. On north Pacific temperature, salinity, sound velocity and density fronts and their relation to the wind and energy flux fields. J. Phys. Oceanogr. 5, 557–571.

Sarnthein, M., Winn, K., Duplessy, J.-C., Fontugne, M.R., 1988. Global variations of surface ocean productivity in low and mid latitudes: influence on CO2 reservoirs of the deep ocean and atmosphere during the last 21,000 years. Paleoceanography 3, 361–399.

Schmiedl, G., Mackensen, A., 1997. Late Quaternary paleoproductivity and deep water circulation in the eastern South Atlantic Ocean: evidence from benthic foraminifera. Palaeogeogr., Palaeoclimatol., Palaeoecol. 130, 43–80.

Schnitker, D., 1974. West Atlantic abyssal circulation during the past 120,000 years. Nature 248, 385–387.

Schnitker, D., 1994. Deep-sea benthic foraminifers: food and bottom water masses. In: Zahn, R., Pedersen, T.F., Kaminski, M.A., Labeyrie, L. (Eds.), Carbon Cycling in the Glacial Ocean: Constraints on the Ocean's Role in Global Change. Springer, New York, pp. 539–554.

Smart, C.W., Gooday, A., 1997. Recent benthic foraminifera in the abyssal northeast Atlantic Ocean: relation to phytodetrital inputs. J. Foraminiferal Res. 27, 85–92.

Smart, C.W., King, S.C., Gooday, A.J., Murray, J.W., Thomas, E., 1994. A benthic foraminiferal proxy of pulsed organic matter paleofluxes. Mar. Micropaleontol. 23, 89–99.

Smith, C.R., Hoover, D.J., Doan, S.E., Pope, R.H., Demaster, D.J., Dobbs, F.C., Altabet, M., 1996. Phytodetritus at the abyssal seafloor across 10° of latitude in the central equatorial Pacific Ocean. Deep Sea Res. II 43, 1309–1338.

Smith, C.R., Berelson, W., DeMaster, D.J., Dobbs, F.C., Hammond, D., Hoover, D.J., Pope, R.H., Stephens, M., 1997. Latitudinal variations in benthic processes in the abyssal equatorial Pacific: control by biogenic particle flux. Deep Sea Res. 44, 2295–2317.

Streeter, S.S., Shackleton, N.J., 1979. Paleocirculation of the Deep North Atlantic: 150,000-year record of benthic foraminifera and oxygen-18. Science 203, 168–171.

Tanaka, Y., 1996. The age analysis based on nannofossil of sediments collected during the NH95-1 cruse (in Japanese). In: Nishimura, A., Kawahata, H. (Eds.), Study on Element Cycles in the Oceans (1995, F.Y. Report). Geological Survey of Japan, pp. 60–74.

Thierstein, H.R., Geitzennauer, K.R., Molfino, B., Shackleton, N.J., 1977. Global synchroneity of late Quaternary coccolith datum levels: validation by oxygen isotopes. Geology 5, 400–404.

Thomas, E., Gooday, A.J., 1996. Cenozoic deep-sea benthic foraminifers: tracers for changes in oceanic productivity? Geology 24, 355–358.

Thomas, E., Booth, L., Maslin, M., Shackleton, N.J., 1995. Northeastern Atlantic benthic foraminifera during the last 45,000 years: changes in productivity seen from the bottom up. Paleoceanography 10, 545–562.

Thompson, P.R., Shackleton, N.J., 1980. North Pacific paleoceanography: late Quaternary coiling variations of planktonic foraminifer *Neogloboquadrina pachyderma*. Nature 287, 829–833.

Thompson, P.R., Bé, A.W.H., Duplessy, J.-C., Shackleton, N.J., 1979. Disappearance of pink-pigmented *Globigerinoides ruber* at 120,000 yr BP in the Indian and Pacific Oceans. Nature 280, 554–558.

Turley, C.M., Lochte, K., 1990. Microbial response to the input of fresh detritus to the deep-sea bed. Palaeogeogr., Palaeoclimatol., Palaeoecol. 89, 3–23.

Ujiié, H., 1990. Bathyal benthic foraminifera in a piston core from east off the Miyako islands, Ryukyu Island Arc. Bull. Coll. Sci., Univ. Ryukyus 49, 1–60.

Ujiié, H., 1995. Benthic foraminifera common in the bathyal surface sediments of the Ryukyu Island Arc region, Northwest Pacific. Bull. Coll. Sci., Univ. Ryukyus 60, 51–111.

van Morkhoven, F.P.C.M., Berggren, W.A., Edwards, A.S., 1986. Cenozoic Cosmopolitan Deep-Water Benthic Foraminifera. Bull. Centr. Rech. Explor. Prod. Elf Aquitaine Mém. 11, 421 pp.

Vella, P., 1962. Late Tertiary nonionid Foraminifera from Wairarapa, New Zealand. Trans. R. Soc. N.Z. 1, 285–296.

Whittaker, J.E., 1988. Benthic Cenozoic Foraminifera from Ecuador. British Museum (Natural History), London, 194 pp.

Xu, X., Ujiié, H., 1994. Bathyal benthic foraminiferal changes during the past 210,000 years: evidence from piston cores taken from seas south of Ishigaki Island, southern Ryukyu Island Arc. Trans. Proc. Palaeontol. Soc. Jpn., N.S. 175, 497–520.

Yasuda, H., 1997. Late Miocene – Holocene paleoceanography of the western equatorial Atlantic: evidence from deep-sea benthic foraminifera. Proc. ODP, Sci. Results 154, 395–431.

Zhang, R.-C., Hanawa, K., 1993. Features of the water-mass front in the northwestern North Pacific. J. Geophys. Res. 98, 967–975.